[redacted]

TNO report
FEL-99-A224

Electric field intensity levels near the HAWK system

(50) 2e expl

TNO Physics and Electronics Laboratory

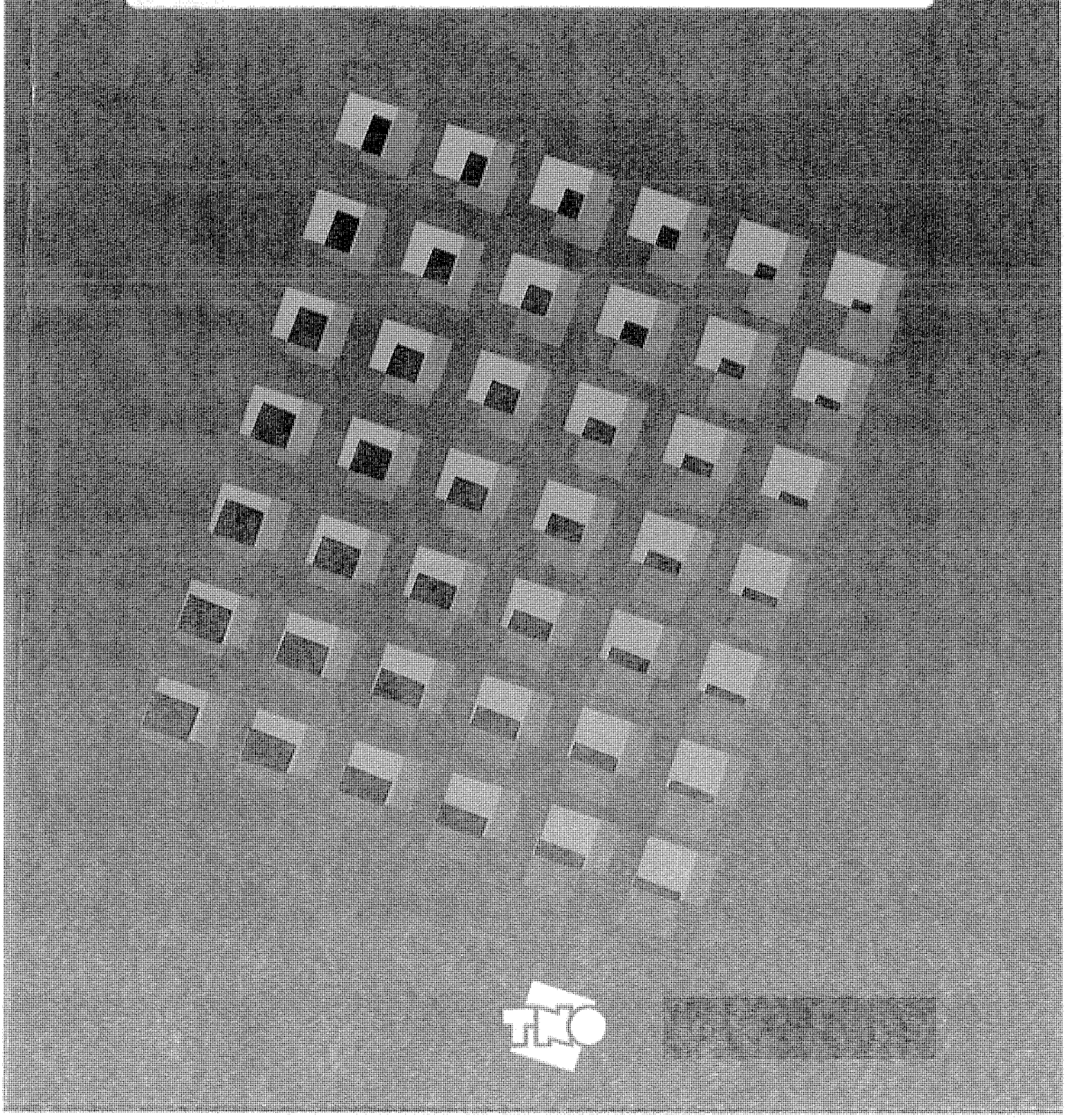

ONGERUBRICEERD

TNO report
FEL-99-A224

Electric field intensity levels near the HAWK system

50/2e expl

TNO Physics and Electronics Laboratory

Oude Waalsdorperweg 63
PO Box 96864
2509 JG The Hague
The Netherlands

Phone +31 70 374 00 00
Fax +31 70 328 09 61

Date
December 1999

Author(s)
[redacted]

Sponsor	Ministerie van Defensie
Project officer	[redacted]
Affiliation	Militair Geneeskundig Facilitair Bedrijf
Classification	
Classified by	[redacted]
Classification date	
Title	Ongerubriceerd
Managementuittreksel	Ongerubriceerd
Abstract	Ongerubriceerd
Report text	[redacted]
Appendices	Ongerubriceerd
Copy no	33
No of copies	66
No of pages	68 (incl appendices, excl RDP & distribution list)
No of appendices	5

ONGERUBRICEERD

The TNO Physics and Electronics Laboratory is part of TNO Defence Research which further consists of:

TNO Prins Maurits Laboratory
TNO Human Factors Research Institute

Netherlands Organization for Applied Scientific Research (TNO)

Managementuittreksel

Titel	:	Electric field intensity levels near the HAWK system
Auteur(s)	:	[redacted]
Datum	:	december 1999
Opdrachtnr.	:	A99D818
IWP-nr.	:	1411
Rapportnr.	:	FEL-99-A224

Doelstelling
Naar aanleiding van berichtgeving over vermeende schadelijke effecten ten gevolge van het werken met de radarsystemen van de HAWK-installaties die door de Koninklijke Luchtmacht werden en worden gebruikt, is de behoefte ontstaan aan het in kaart brengen van de elektrische veldsterkten in de directe omgeving van deze radarsystemen. Deze veldsterkten zijn maatgevend voor de intensiteit van de zogenoemde radarstraling. Aan de hand van de waarden van deze veldsterkte kunnen op relevante locaties op een HAWK-site, onder operationele omstandigheden, veilige afstanden worden vastgesteld die zijn afgeleid uit de blootstellingslimieten gegeven in de tweede editie van STANAG 2345 (edition-2, 1997).

Omschrijving van de werkzaamheden
Voor het in kaart brengen van de optredende elektrische veldsterkte nabij een HAWK-installatie is een meetprotocol opgesteld. Op basis van dit meetprotocol zijn in december 1998 door TNO-FEL veldsterktemetingen uitgevoerd nabij radars van de HAWK-installatie die stonden opgesteld op de vliegbasis Twenthe. Deze radars waren de CWAR en de HIPIR. De ruwe meetgegevens zijn uitgewerkt en geschikt gemaakt voor grafische presentatie. Om een compleet beeld te krijgen zijn in aanvulling op de metingen berekeningen uitgevoerd teneinde de elektrische veldsterkten op tussenliggende en grotere afstanden te kunnen berekenen. Tot slot is een vergelijking gemaakt tussen de gemeten en berekende waarden.

Conclusies
De berekende waarden van de veldsterkte sluiten goed aan bij de verkregen meetresultaten. Deze meetresultaten tonen aan dat, op de door de Koninklijke Luchtmacht gehanteerde veiligheidsafstanden tot de CWAR en de HIPIR, wordt voldaan aan de in de tweede editie van STANAG 2345 (edition-2, 1997) gegeven blootstellinglimieten.
Hierna wordt gedetailleerder op de resultaten voor de beide radarsystemen ingegaan.

Blootstelling aan door de CWAR opgewekte elektrische velden
Uitgaande van de hoogte van het centrum van de zendantenne van 2,77 m boven het maaiveld volgt uit berekeningen en metingen dat ongeacht de afstand tot de antenne binnen een hoogte van 1,90 m boven het maaiveld continu verblijf is toegestaan indien de elevatiehoek van de CWAR-antenne geen negatieve waarden aanneemt, dat wil zeggen niet naar beneden is gericht. Dit geldt zowel voor een roterende als voor een stilstaande CWAR-antenne. Uit berekeningen volgt dat in de hoofdbundel van de CWAR-antenne, op afstanden groter dan [redacted] m, continu verblijf conform de tweede editie van STANAG 2345 (edition-2, 1997) is toegestaan. De momenteel door de Koninklijke Luchtmacht gehanteerde veiligheidsafstand van 36 m voldoet hieraan.

Blootstelling aan door HIPIR opgewekte elektrische velden
De momenteel door de Koninklijke Luchtmacht gehanteerde veiligheidsafstand tot de HIPIR-antenne bedraagt 111,5 m. Deze afstand is gebaseerd op blootstelling in de hoofdbundel. De op de vliegbasis Twenthe uitgevoerde metingen, op afstanden groter of gelijk aan deze veiligheidsafstand, tonen geen overschrijding van de in de tweede editie van STANAG 2345 (edition-2, 1997) gegeven limieten, voor continue blootstelling van het gehele lichaam of delen ervan, aan. Berekeningen onder 'worst case' conditie (volledige bodemreflectie) tonen aan dat op afstanden van 111,5 m en groter aan de blootstellingslimieten wordt voldaan voor continue blootstelling van het gehele lichaam en delen van het lichaam, met uitzondering van de ogen. Speciale aandacht moet aan de ogen worden gegeven omdat hiervoor een lagere blootstellingslimiet geldt in verband met een geringere bloedcirculatie.

Contents

List of symbols and abbreviations 7

1. Introduction 9

2. Radio frequency radiation safety standards 11
   - 2.1 Introduction 11
   - 2.2 ICNIRP guidelines 12
   - 2.3 Health Council of the Netherlands 13
   - 2.4 STANAG 2345 13

3. HAWK system 15
   - 3.1 Introduction 15
   - 3.2 HIPIR 15
   - 3.3 CWAR 16
   - 3.4 IFF system 16
   - 3.5 HAWK installation at Twenthe Air Base 17

4. Theoretical approach 19
   - 4.1 Introduction 19
   - 4.2 Field regions 19
   - 4.3 Electric field calculations 20
   - 4.4 Ground reflections 21

5. Theoretical results 25
   - 5.1 HIPIR theoretical results 25
   - 5.2 CWAR theoretical results 34
   - 5.3 IFF calculations 35

6. Measurements 41
   - 6.1 Measurement equipment and software 41
   - 6.2 Individual radar measurements 42
   - 6.3 HAWK installation measurements 44
   - 6.4 Measurement results 45

7. Conclusion 51
   - 7.1 HIPIR 51
   - 7.2 CWAR 52

8. References 53

9. Signature 55

Appendices
- A Field calculation
- B Reflection on plane boundaries

C	Rough surface criteria
D	Determination of aperture illumination
E	Measurement errors

List of symbols and abbreviations

A	Ampere, unit of electric current
A/m	Ampere per meter, SI unit of magnetic field strength
ANSI	American National Standards Institute
CW	Continuous Wave
CWAR	Continuous Wave Acquisition Radar
D	Average depth of irregularity
D	Diameter of antenna
d	Distance from the source in m
dB	Decibel
D band	Frequency band between 1 GHz and 2 GHz
E	Electric field strength
E_i	Value of the internal electric field strength in the body tissue in V/m
E_{rms}	Root mean square value of the electric field averaged in a height interval
ELF	Extremely Low Frequency
EM	Electromagnetic
EMF	Electromagnetic Field
FM	Frequency Modulation
G_i	Antenna far-field gain relative to an isotropic radiator
GEN	Generator
GHz	Giga Hertz (1000 MHz)
H	Magnetic field strength
HAWK	Homing All the Way Killer
HIPIR	High Powered Illuminator Radar
Hz	Hertz (one Hertz equals one cycle per second)
ICNIRP	International Commission on Non-Ionising Radiation Protection
IFF	Identification Friend or Foe
INIRC	International Non-Ionising Radiation Committee
IRPA	International Radiation Protection Association
ITU	International Telecommunications Union
J band	Frequency band between 10 GHz and 20 GHz
kHz	Kilo Hertz (1000 Hz)
kW	Kilo Watt (1000 W)
LSCB	Launcher Section Control Box
m	meter, unit of length
MHz	Mega Hertz (1000 kHz)
NIR	Non-Ionising Radiation
NLR	National Aerospace Laboratory
P	Mean output power in W
PCP	Platoon Command Post

P_d	Power density
PEL	Permissible Exposure Level
RF	Radio Frequency
RFR	Radio Frequency Radiation
rms	Root mean square
s	Second, unit of time
S	Siemens, unit of conductance
SAR	Specific Absorption Rate
SI	Système International
STANAG	NATO Standardisation Agreement
VHF	Very High Frequency
V/m	Volt per meter, unit of electric field strength
W	Watt, unit of power
W/kg^{-1}	Watt per kilogram
W/m^2	Watt per square meter, SI unit of power density
Z_0	Impedance of free space, equals $120\pi\ \Omega$ or $377\ \Omega$
ε	Permittivity [SI unit: F/m]
λ	Wavelength [SI unit: m]
ρ	Mass density [SI unit: kg/m^3]
σ	Electrical conductivity [SI unit: S/m]
Ω	Ohm, unit of impedance

1. Introduction

Due to concern among Airforce personnel about the supposed relationship between health disorders and the exposure to electromagnetic fields due to radiators of the HAWK system, TNO-FEL was sponsored by the Netherlands Defence organisation to investigate the electric field intensities on the site of a HAWK installation.

The results of this investigation are presented in this report.
Because of the large amount of measurement data, the complete set of measurement results has been entered in a separate document named: 'HAWK measurement results'.
In Chapter 2 of this report the most important safety standards are mentioned in which exposure limits are defined. Chapter 3 gives a brief description of the HAWK installation and its relevant technical specifications, necessary for the theoretical analysis. Chapter 4 deals with the theoretical approach for field calculations which leads to the theoretical results presented in Chapter 5 where electric field intensities are presented by several graphs.
Chapter 6 describes the measurement procedure and the measurement results, which are compared with the theoretical values. Finally in Chapter 7 the conclusions are formulated.
Five appendices are added to this report, which give more detailed technical background information.

[redacted]

2. Radio frequency radiation safety standards

2.1 Introduction

The radio frequency portion of the electromagnetic spectrum extends over a wide range of frequencies, from about 10 kHz to 300 GHz. In the last two or three decades, the use of devices that emit radio frequency radiation (RFR) has increased dramatically. The proliferation of RF devices has been accompanied by increased concern about the safety of their use. This concern, in turn, has led to increased RFR research (resulting in a much better understanding of the interaction of RFR fields and biological systems) and to new RFR safety guidelines. The present exposure standards are based on what is known about the frequency-dependent nature of RFR energy deposition in biological systems and about any biological effects. In general dosimetric quantities are needed to estimate the absorbed energy and its distribution inside the body. A dosimetric quantity that is widely adopted for the frequency range from 100 kHz to 300 GHz is the Specific Absorption Rate (SAR), defined as the time derivative of the incremental energy, absorbed by or dissipated in an incremental mass contained in a volume element of a given density. SAR is expressed in the unit watt per kilogram (W/kg).
Local SAR is given by:

$$SAR = \frac{\sigma E_i^{\,2}}{\rho} \tag{2.1}$$

where σ is the electric conductivity, E_i is the internal electric field strength in the body tissue and ρ the mass density of the body tissue. In practice SAR is always determined as an average value in the finite tissue volume. The whole body average SAR, simply gives the power absorbed into the whole human body divided by the mass of the body. It can be seen from Equation (2.1) that SAR is directly related to the conductivity of the tissue. SAR is the dosimetric unit of biological effects associated with the temperature increase in tissue. However, also the electric field strength can be used as a dosimetric unit particularly when effects of other type are concerned. Microwave energy absorption occurs at the molecular, cellular, tissue and whole-body levels. The dominant factor for net energy absorption by an entire organism is related to the dielectric properties of tissue types, which ultimately causes conversion of electromagnetic energy into heat. The amount of heat transferred to a biological system is important for the purpose of distinguishing those cases where the biological system may be affected by a change in temperature from those where the energy is too little or too dispersed to cause any noticeable change in temperature. For laboratory experiments, exposure conditions can be classified in three categories: thermal, a-thermal, and non-thermal. In the thermal regimen, the core temperature of the organism may rise by up to 5 °C, in spite of thermal regulation. In the a-thermal range, thermal regulation maintains the organisms temperature at its nominal value. Under non-thermal conditions, there is no challenge to thermal regulation or change in organism

temperature. There is currently a general consensus in the scientific and standards community that the most significant parameter, in terms of biological relevant effects of human exposure to radio frequency electromagnetic fields, is the SAR in tissue. The setting of safety limits for human exposure to RFR fields is performed in two steps. First basic limits for SAR inside the body are specified, then relationships between SAR values and unperturbed field strengths are used to set derived limits for field strength and power density. It is assumed that in humans exposure to an average whole body SAR of 2 W/kg – 4 W/kg during minimally 20 to 30 minutes leads to a total body warming in the order of 0,5 °C. A sustained 1 °C temperature rise in core body temperature is generally accepted to be the maximum tolerable. Based on this and animal experiments all guidelines proposing organisations feel that exposure to EM fields should not lead to a averaged whole body SAR of more than 4 W/kg. To this value safety factors are often applied. The following guidelines are currently in use in the Netherlands: ICNIRP guidelines, the recommendations of the Health Council of the Netherlands, both for the general public and for workers and STANAG 2345 (edition-2, 1997) for military use. These guidelines are summarised in the following Sections.

2.2 ICNIRP guidelines

In 1974, the International Radiation Protection Association (IRPA) formed a working group on Non-Ionising Radiation (NIR), which examined the problems arising in the field of protection against the various types of NIR. At the IRPA Congress in Paris in 1977, this working group became the International Non-Ionising Radiation Committee (INIRC). At the Eight International Congress of the IRPA (Montreal, 18-22 May 1992), a new independent scientific organisation, the International Commission on Non-Ionising Radiation Protection (ICNIRP), was established as a successor to the IRPA/INIRC. The task of the Commission is to investigate the hazards that may be associated with the different forms of NIR, to develop international guidelines on NIR exposure limits and to deal with all aspects of NIR protection. As mentioned before several studies of thermal regulatory responses of resting volunteers exposed to RFR have demonstrated that exposure for up to 30 min, under conditions in which average whole body SAR was less than 4 W/kg, caused an increase in the body core temperature of less than 1 °C. An average whole body SAR of 0,4 W/kg has therefore been chosen as the restriction that provide adequate protection for occupational exposure. An additional safety factor of 5 is introduced for exposure of the public, giving an average whole body SAR limit of 0,08 W/kg. Table 2.1 summarises the reference levels for occupational exposure and exposure of the general public.

Table 2.1: ICNIRP Exposure limits in the frequency range from 2 GHz to 300 GHz

ICNIRP Exposure limits			
	Electric field [V/m]	Magnetic field [A/m]	Power density [W/m^2]
Occupational	137	0,36	50
General public	61	0,16	10

2.3 Health Council of the Netherlands

In 1997 the Health Council of the Netherlands issued new recommendations for maximum acceptable exposure to radio frequency electromagnetic fields. The title of this advisory report is 'Radiofrequency electromagnetic fields (300 Hz - 300 GHz)'. The effects of exposure to electromagnetic fields differ, depending on the frequency of the fields. The exposure limits which are derived from the basic restrictions are for the frequency of interest (10 GHz) given in Table 2.2. In this table a distinction is made between workers and the general public. Workers are supposed to be exposed only during working hours, while the general public can be exposed continuously.

Table 2.2: Health Council proposed maximum electric field strengths for the frequency range from 2 GHz -10 GHz

Health Council of the Netherlands	
	Electric field [V/m]
Occupational	194
General public	87

2.4 STANAG 2345

Edition 2 of the Nato Standardisation Agreement (STANAG) 2345 is issued in 1997. The title is 'Evaluation and Control of Personnel Exposure to Radio Frequency fields – 3 kHz to 300 GHz'. This RF protection standard is primarily based, as the other standards, on the specific absorption rate. The permissible exposure levels listed in Table 2.3 refer to values averaged over any 6-minute period and are expressed as a power density. For ease of comparison with the other standards also the calculated equivalent (far field) electric field strength has been given.

Table 2.3: STANAG 2345 permissible exposure levels

STANAG 2345 permissible exposure levels		
Frequency range [GHz]	Power Density [W/m^2]	Electric field [V/m]
0.3 – 3	f/30*)	
3 – 15	100	194

*) f in MHz

In nonuniform fields, the spatial rms peak values could exceed the Permissible Exposure Level (PEL) even though the spatially averaged rms value does not exceed the PEL. The spatial rms peak value is limited to 200 $(f/6000)^{0.25}$. For the frequencies under consideration (10 GHz) the value is 227 W/m^2 (293 V/m). This relaxation is only allowed for partial-body exposure of all parts of the body except for the eyes. The exposures to the eyes are limited by the basic exposure criteria of a whole-body averaged SAR of 0.4 W/kg, corresponding to 194 V/m.

For determining safety distances with respect to radars, exposure limits mentioned in STANAG 2345 are used by the Royal Netherland Airforce.

3. HAWK system

3.1 Introduction

To compare the electric field intensity generated by the HAWK radiators to the exposure limits mentioned in the previous chapter, a field intensity analysis can be made. A necessary first step in performing the analysis is to obtain information on the specifications of the individual electromagnetic sources (radiators). The HAWK system as used by the Royal Netherlands Airforce at Twenthe Air Base consists of the following electromagnetic sources:

- High Power Illuminator Radar (HIPIR),
- Continuous Wave Acquisition Radar (CWAR),
- Identification Friend or Foe (IFF).

The content of this chapter will deal with the relevant specifications of these sources. A situation sketch of the HAWK set-up at Twenthe Air Base will be given in Section 3.5.

3.2 HIPIR

3.2.1 Description

The HIPIR is a J band radar developed to automatically track and illuminate targets. It provides missiles with a reference signal and supplies pre-launch signals to position the launcher in azimuth and elevation [1]. Because of the HIPIR's tracking features, negative main-beam elevation angles can occur. The main-beam's elevation angle is not fixed (contrary to the CWAR's main-beam elevation angle). Both elevation and azimuth angles depend on the direction of the illuminated target.

3.2.2 Specifications

Some relevant technical specifications of the HIPIR's pencil-beam transmit system are listed below:

Transmit antenna:
Height to centre of antenna:
Vertical dim. antenna aperture:
Diameter:
Antenna gain G_i:
Radiated power:
Frequency:
Duty cycle:
Beamwidth (3 dB):
Polarisation:

[redacted]

3.3 CWAR

3.3.1 Description

The CWAR is a radar that is developed to detect low-altitude targets in the presence of high-level ground clutter. Moving targets are detected in speed through an application of the doppler principle. CW signals and FM/CW signals are transmitted on alternate rotations of the CWAR antenna [1]. When operating, the radar's antenna rotation rate amounts [redacted] rotations per minute. The main-beam's elevation angle is fixed and normally set to 0 degrees.

3.3.2 Specifications

Some relevant technical specifications of the CWAR's transmit system are listed below:

Transmit antenna:
Height of centre of antenna:
Vert. dim. antenna aperture:
Hor. dim. antenna aperture:
Antenna gain G_t:
Radiated power:
Frequency:
Duty cycle:
Vertical beamwidth (3 dB):
Horizontal beamwidth (3 dB):
Polarisation:
Rotation rate:

[redacted]

3.4 IFF system

3.4.1 Description

IFF is used to identify targets detected by the CWAR. The IFF system can be installed on top of the Platoon Command Post (PCP), a tripod or a mast.

3.4.2 Specifications

Some relevant technical specifications of the IFF transmit equipment are given below:

Frequency:
Antenna gain G_t:
Radiated power:

[redacted]

3.5 HAWK installation at Twenthe Air Base

In Figure 3.1 the HAWK installation at Twenthe Air Base is shown. Abbreviations in the figure are explained in the list of symbols and abbreviations.

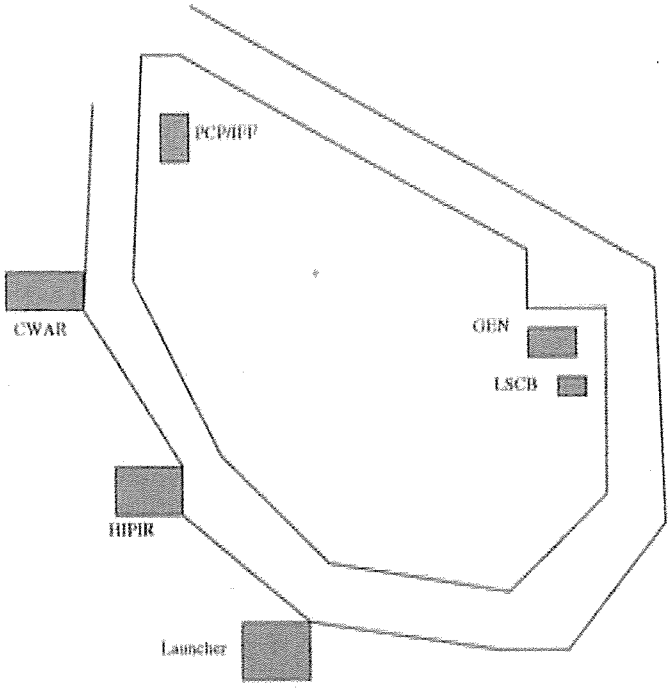

Figure 3.1: Plan of HAWK installation at Twenthe Air Base (not on scale)

4. Theoretical approach

4.1 Introduction

Because results obtained by measurements are liable to uncertainties like environmental conditions, measurement errors and fluctuations in radiated power, it is necessary to obtain theoretical information. Using the technical electromagnetic source specifications of the previous chapter a theoretical analysis can be performed.
The strategy for the theoretical analysis runs as follows:

1. Determination of the antenna's aperture illumination (necessary for calculations).
2. Calculation of the electric field intensity at several distances within the main-beam and out of the main-beam (for example below the main-beam).
3. Calculations of the electric field intensity at several distances from the source, taking ground reflections into account.

Information on electric field intensities within the main-beam is available in the literature [2], [3] and [4] for various aperture illuminations (field distribution in the antenna opening). Information, however, on fields generated out of the main-beam is of importance as well, because, maximum field intensities do not necessarily occur within the main-beam. Besides, out of the main-beam fields have to be considered when ground reflections are taken into account. To fill up these lacking information, software, based on the theory of Section 4.3 has been developed to determine field intensities within the main-beam as well as in any point out of the main-beam.

4.2 Field regions

The important regions of radiation associated with a large aperture antenna are the Fresnel (radiating near-field) and the far-field regions. In the Fresnel region the beam is formed and both the antenna gain and beamwidth vary with the type of antenna illumination and the distance from the antenna. Beyond the radiating near-field region the far-field region starts where beamwidth (in degrees) and gain are independent of the distance. In this region the field strength in the main-beam can be expressed by:

$$E = \sqrt{\frac{Z_0 P G_i}{4\pi r^2}} \tag{4.1}$$

in which:

E = Electric field strength [V/m],
P = Mean output power [W],
G_i = Far-field antenna power gain relative to an isotropic radiator,
r = Distance from antenna in the far-field region [m],
Z_0 = Impedance of free space = 377 Ω.

Because maximum exposure field intensity levels can arise in the Fresnel region the field analysis must cover this region. In this region however, Equation (4.1) is inaccurate and has to be corrected for near-field effects.

4.3 Electric field calculations

The near-field corrections for gain and beamwidth depend on the type of antenna aperture illumination (field distribution in the antenna opening, Figure 4.1) and the distance from the antenna [1], [3], [4]. Specification of the aperture illumination is therefore necessary to be able to conduct field calculations. If the antenna aperture illumination is unknown, it can be estimated by the 3 dB (far-field) beamwidth using the method described in Appendix D.

Field calculations in and out of the main-beam can be performed using the equivalence principle. Actual sources in medium 1, responsible for the field distribution in the antenna aperture are replaced by fictitious equivalent dipole sources in the antenna aperture, such that they produce the same fields within the region of interest (medium 2) as illustrated in Figure 4.1. Regarding the aperture now as a continuous array of electric and magnetic dipoles, the field intensity in medium 2 can be calculated. The results are scaled to fulfil Equation (4.1) in the far-field using the manufacturer specified P (power) and G_i (gain).
Details concerning the calculations can be found in Appendix A.

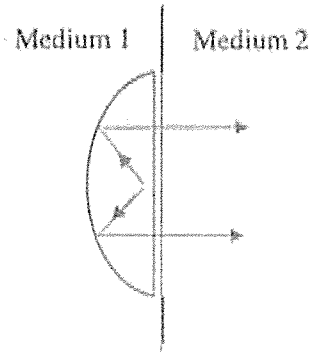

Figure 4.1: Side view of antenna aperture (dashed vertical line)

4.4 Ground reflections

Depending on the texture of the reflecting surface two types of ground reflection can be distinguished: specular and diffuse reflection. Specular reflection is a reflection caused by a smooth surface: it is directional and it obeys the laws of classical optics and its phase is coherent. The laws for reflection on planar boundaries, summarised in Appendix B, can be used. Diffuse scattering, however, is a phenomenon that is dominant in case of reflection on rough surfaces. It has little directivity, its phase is incoherent and its fluctuations are large in amplitude. In case of a smooth surface the specular reflected wave can be modelled as coming from a virtual mirror source having an attenuation and phase shift depending on the reflection coefficient of the ground surface. The electric field at a point P, can be obtained by the summation of direct and reflected wave contributions. If the amplitude of the reflected field is comparable to that of the directly propagated field, deep fades of the resultant field through destructive interference can be produced.
For rough surfaces both specular and diffuse reflection occur. The diffusely scattered field, which amplitude is usually smaller, produces, when interfering with the direct ray, more rapid and less deep fading [5].

4.4.1 Smooth surface reflection model: HIPIR

Because the elevation angle θ of the HIPIR can take negative values, Figure 4.2 shows (for a smooth surface) the direct and reflected wave for a HIPIR directed downwards to point Q(d,h_2) at a distance d from the HIPIR and at a height h_2 above the surface. Point P(d,h_1) is defined as the point were the electric field is calculated. The electric field in point P(d, h_1) is given by the superposition of direct and indirect wave contributions. The amplitude of the total field follows from:

$$E_{Total}(d,h_1) = E_{direct}(d,h_1) + E_{reflected}(d,h_1) = \\ E(R_1,\beta_1) + \rho(\psi,\varepsilon,\sigma)E(R_2,\beta_2) \tag{4.2}$$

and

$$|E_{Total}(d,h_1)| \le |E_{direct}(d,h_1)| + |E_{reflected}(d,h_1)| \tag{4.3}$$

In case of constructive interference, that is direct and reflected wave add in phase, the electric field intensity becomes:

$$|E_{Total}(d,h_1)| = |E_{direct}(d,h_1)| + |E_{reflected}(d,h_1)| \tag{4.4}$$

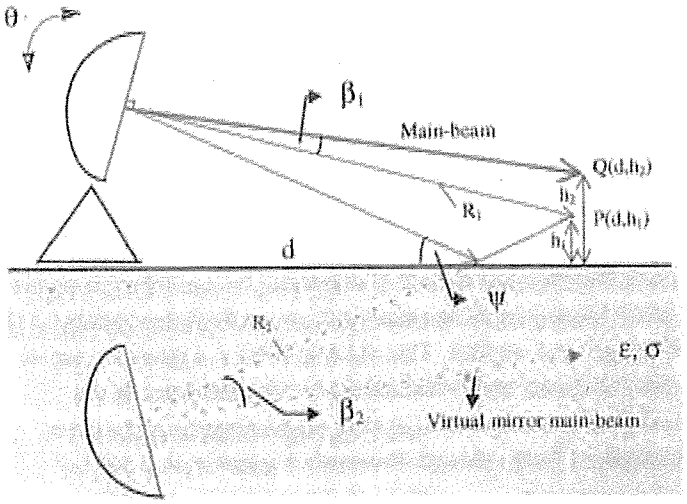

Figure 4.2: Direct and reflected waves for a HIPIR directed to point Q(d, h_2) at a distance d from the HIPIR and at a height h_2 above the surface. Point P(d, h_1) is defined as the point were the electric field is calculated. θ is the elevation angle.

4.4.2 Smooth surface reflection model: CWAR

In case of a smooth surface,

Figure 4.3 displays the geometry of the CWAR for 0 degrees elevation angle with direct and reflected waves propagating to point P(d,h_1) (at distance d from the CWAR and at a height h_1 above the ground surface).

The electric field in point P(d, h_1) can be calculated by the summation of direct and indirect wave contributions:

$$E_{Total}(d,h_1) = E_{direct}(d,h_1) + E_{reflected}(d,h_1) = E(R_1,\beta_1) + \rho(\psi,\varepsilon,\sigma)E(R_2,\beta_2) \tag{4.5}$$

For constructive interference (direct and reflected wave add in phase) the electric field intensity becomes:

$$\left|E_{Total}(d,h_1)\right| = \left|E_{direct}(d,h_1)\right| + \left|E_{reflected}(d,h_1)\right| \tag{4.6}$$

in which:

d: Distance from CWAR [m],

h_1: Height above ground [m],

β_1: Out of main-beam angle [radian],

β_2: Out of reflected main-beam angle [radian],

R_1: Path length direct ray to point (d, h_1) [m],

R_2: Path length reflected ray to point (d, h_1) [m],
ψ: Grazing angle [radian],
ρ: Reflection coefficient,
σ: Conductivity ground [S/m],
ε: Permittivity of ground [F/m].

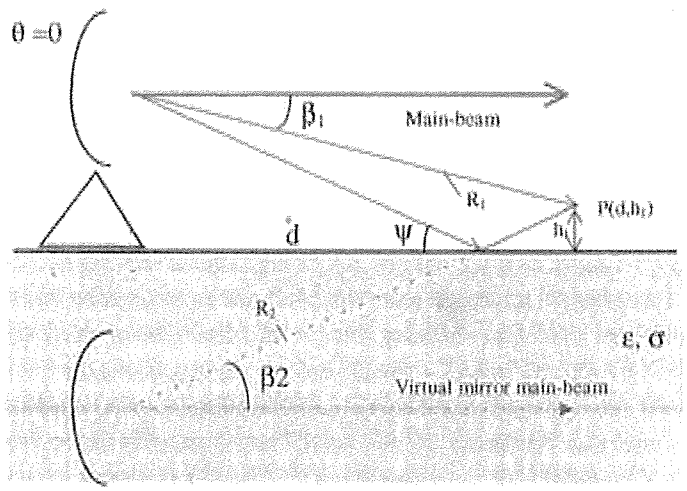

Figure 4.3: Direct and reflected wave for a CWAR having an elevation angle $\theta = 0$ degrees.

4.4.3 Smooth surface reflection coefficient

In Appendix B it is shown that the reflection coefficient of a plane ground surface depends on the polarisation of the electric field, the grazing angle of the incident wave and the electrical characteristics of the earth. In the ITU recommendations 527-3 [6], electrical characteristics of the earth are specified. Some of them are given in Table 4.1. Using these specifications the reflection coefficient $\rho(\psi, \varepsilon, \sigma)$ can be calculated. Because the reflection coefficient is dependent on the polarisation of the incident wave it is important to notice that the HIPIR and the CWAR generate respectively vertical and horizontal polarised waves.

Table 4.1: Ground parameters (from [6])

Description	ε_r	σ (S/m)
Wet ground	12	3.0
Medium dry ground	12	1.4
Very dry ground	3	0.045
Ice -1 °C	3	0.0054
Ice -10 °C	3	0.0017

4.4.4 Surface irregularity

When the electromagnetic wave is incident on a plane interface between two media, the plane will reflect the incident wave specularly in a single direction and reflection can be described by the laws summarised in Appendix B.
However, if the boundary is not plane but rough, the boundary will reflect the incident wave in various directions (diffuse scattering). Besides, due to the irregularity of the surface, phase differences occur between reflected rays. The Rayleigh criterion (Appendix C) establishes an approximate dividing line for the average depth of irregularity between truly rough surfaces and those that may be regarded as smooth. The dividing line is based on a maximum phase shift that can occur due to reflected waves propagating to a point.

5. Theoretical results

5.1 HIPIR theoretical results

The beamwidth of the HIPIR antenna and the diameter indicate, using the criteria of Appendix D, that the illumination in the antenna aperture can be regarded as a $1-(2r/D)^2$ shaped electric field distribution in which r is the distance to the centre of the aperture and D is the diameter of the antenna [2]. To estimate the generated electric field, calculations have been made assuming the technical specifications of Section 3.2.2.

5.1.1 Smooth surface reflection

Because the elevation angle of the HIPIR can take negative values, the influence of ground reflections on the field intensity has to be investigated. To do this, the reflectivity is calculated for several ground conditions assuming an incident plane wave with grazing angle ψ (see Figure 4.2) and electric field vector in the plane of incidence (vertical polarisation, Appendix B, Figure B.1). The amplitude and the phase of the reflection coefficient can be visualised as a function of the grazing angle as shown in Figure 5.1 and Figure 5.2. At a frequency of 10 GHz the reflection coefficient is determined by the conductivity σ of the ground. Wet ground and medium dry ground have nearly the same reflection coefficients just as very dry ground and ice have. For small grazing angles the absolute value of ρ, independently of the ground parameters approaches 1 and the phase shift amounts to 180 degrees.

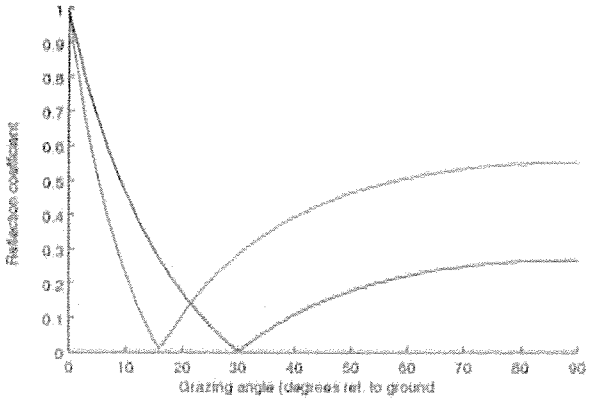

Figure 5.1: Reflection coefficient at 10 GHz, for E vector in plane of incidence
Red: Wet ground, medium dry ground
Black: Very dry ground, Ice

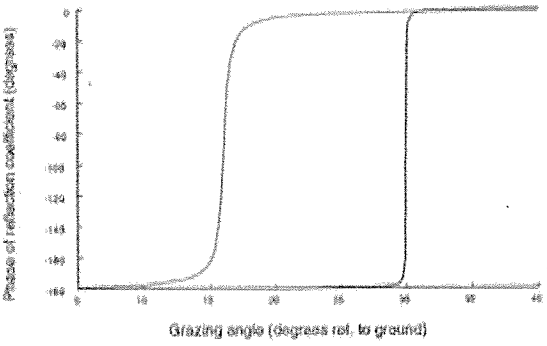

Figure 5.2: Reflection coefficient phase at 10 GHz, for E vector in plane of incidence
Red: Wet ground, medium dry ground
Black: Very dry ground, Ice

5.1.2 Surface irregularity

Figure 5.3 shows the maximum average surface irregularity to regard the surface as smooth, versus the distance of a field point (at which the field is calculated) at 1.5 m above the surface (see Appendix C). The calculation is based on the grazing angle of a ray radiated from the HIPIR and reflected via the surface to a point P(d,h=1.5) at distance d from the HIPIR and height 1.5 m above the surface. If the surface irregularity is smaller than indicated in Figure 5.3, specular reflection dominates and the flat surface approach of Appendix B is valid as well as the reflection coefficients calculated in Section 5.1.1. If the surface irregularity is larger than indicated in Figure 5.3, diffuse reflection dominates. Considering field intensities at distances between 100 m and 200 m Figure 5.3 shows that the surface can be regarded as flat if the average surface irregularity is smaller than approximately 3 cm. Because at Twenthe Air Base parts of the surface consist of asphalt, these parts can be regarded to be flat. So, the 'worst case' calculations in this chapter will be based on a flat surface assuming constructive interference.

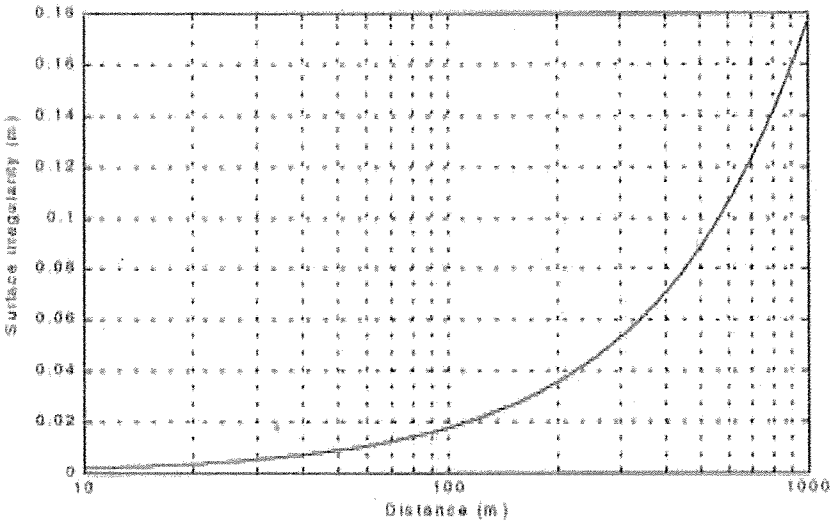

Figure 5.3: Maximum surface irregularity (π/8 phase criterion) to regard the surface as smooth.
Calculation based on the grazing angle of a ray radiated from the HIPIR and reflected via the surface to a point P(d,h=1.5) at distance d from the HIPIR and height h= 1.5 m above the surface.

5.1.3 HIPIR calculations

From section 5.1.2 and Appendix C it follows that the asphalt for low grazing angles can be regarded as a flat surface and the absolute value of the reflection coefficient amounts to 1 (maximum reflection) independent of the ground type. Therefore we apply a worst case analysis by using a perfectly conducting flat ground plane (which gives complete reflection for all grazing angles) in the calculations and assume constructive interference (direct and reflected waves add in phase). Electric field calculations were made for the following situations:

1. In the first situation the electric field has been calculated at points P(d,h) corresponding to distances of 20 m < d < 1000 m and heights of h = 0 m, 0.5 m, 1 m, 1.5 m and 1.9 m, while the main-beam of the HIPIR antenna was directed to the same points Q(d,h) = P(d,h). So the point in which the field is calculated is the same point as the point to which the HIPIR is directed.
2. In the second situation, calculations were performed at the same points P(d,h) as for the first situation while the HIPIR antenna was directed to points Q(d,h=0m) at the ground surface (h = 0 m).

The first situation gives larger electric field intensities at smaller distances, while the second situation gives larger field intensity levels for larger distances. As the distance becomes larger, electric field values from both situations approach each other. The results for situation 1 (field point is point to which HIPIR antenna is directed) are plotted in Figure 5.4 and

Figure 5.5. For lines 1 to 5 constructive interference was assumed (direct and reflected waves add in phase) for a perfectly conducting ground. Line B represents the intensity of the direct wave only (without ground reflection). Because in reality direct and reflected rays don't add in phase at all locations, fading occurs (variation in field intensity as a function of phase difference between direct and reflected waves). As an example this is shown by line A which gives the situation for dry ground at field points 1.9 m above ground. The envelope of line A is slightly below line 5, which represents the situation for a *perfectly conducting* ground (and constructive interference). The results for situation 2 (HIPIR antenna pointed to Q(d,h=0m) are presented in
Figure 5.6 and Figure 5.7. For distances larger than approximately 100 m, the field intensity levels at heights smaller than or equal to 1.9 m are larger for situation 2 than for situation 1. In Figure 5.8 the electric field intensity at 111.5 m from the HIPIR (the present safety distance used by the Royal Netherlands Airforce) is presented as a function of the height.

5.1.4 Conclusion theoretical results HIPIR

From the results plotted in Figure 5.4,
Figure 5.5,
Figure 5.6 and Figure 5.7 it follows that the electric field intensity in a point depends on its distance from the HIPIR, its height above the ground and the direction of the HIPIR antenna.
At the moment the HIPIR safety distance as used by the Royal Netherlands Airforce amounts 111.5 m.
From the results of Figure 5.8 it follows that at that distance, in a worst case situation assuming a flat, perfectly reflecting, ground and constructive interference, the calculated electric field intensity locally can have values of maximal [redacted] V/m for heights between 0.0 m and 1.9 m. Only for heights lower than 0.03 m the PEL of STANAG 2345 for partial body exposure is exceeded. Due to the small height and the small crossing (3V/m) of the exposure limit this interval will not be considered. Because of fading, however, the average electric field intensity E_{rms} (root mean square value averaged in the height interval from 0 m to 2 m) will be smaller and amounts [redacted] V/m (Figure 5.8) for the HIPIR antenna directed to point P(d=111.5m, h=0m).
According to STANAG 2345 (edition-2, 1997) these electric field values indicate that at a distance of 111.5 m a whole body exposure (except for the eyes) is permitted without time restriction (see section 2.4). For the eyes an exposure restriction applies of maximum 2.6 minutes exposure per any arbitrary period of 6-minutes (assuming zero exposure during the remaining 3.4 minutes).

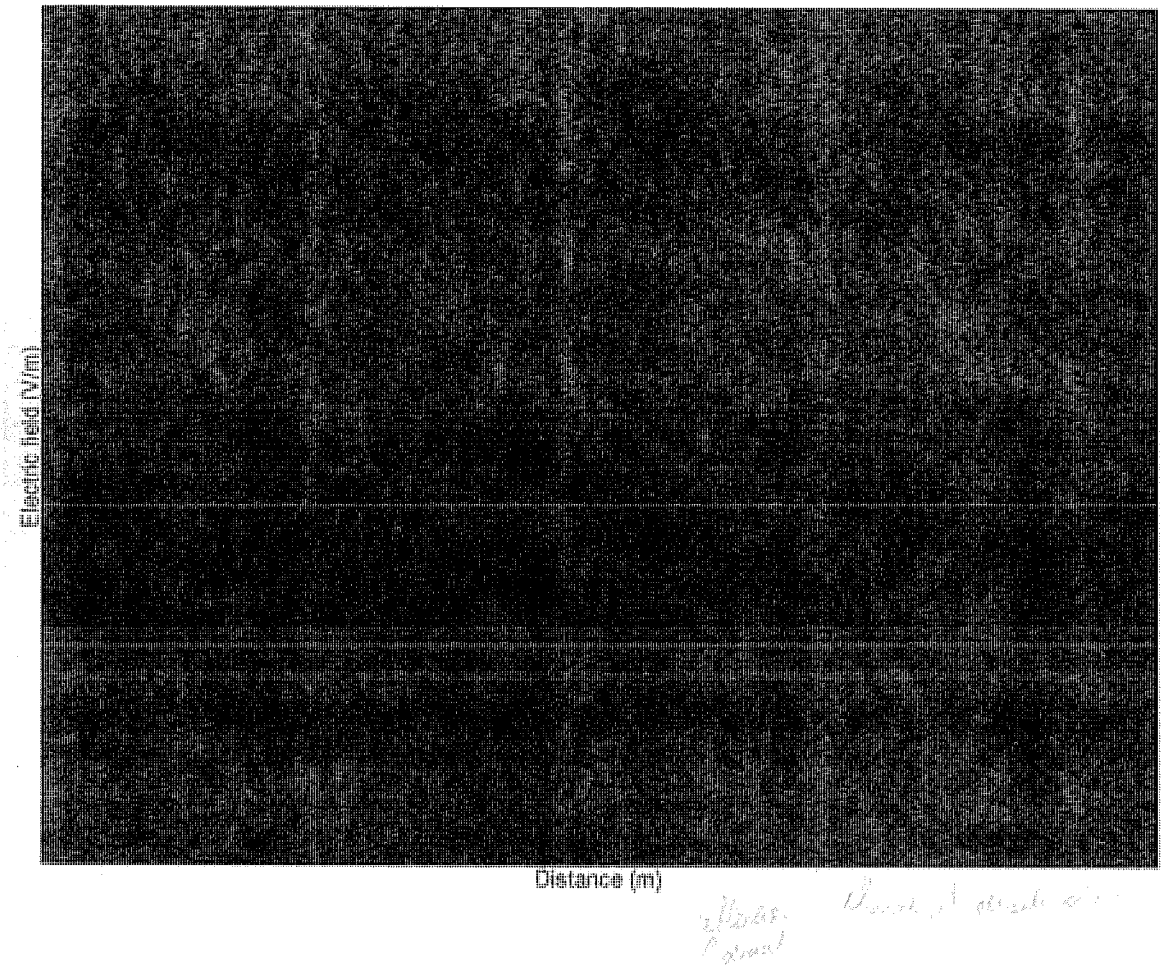

Figure 5.4: *Theoretic electric field intensity E in point P(d,h) at distance d and height h while HIPIR is directed to point P(d,h). (constructive interference and perfect reflection assumed except for Line A).*

Line 1: |E *direct*| + |E *reflected*| *at h = 0 m (perfectly conducting ground)*
Line 2: |E *direct*| + |E *reflected*| *at h = 0.5 m (perfectly conducting ground)*
Line 3: |E *direct*| + |E *reflected*| *at h = 1.0 m (perfectly conducting ground)*
Line 4: |E *direct*| + |E *reflected*| *at h = 1.5 m (perfectly conducting ground)*
Line 5: |E *direct*| + |E *reflected*| *at h = 1.9 m (perfectly conducting ground)*
Line A: |E *direct* + E *reflected*| *at h = 1.9 m (dry ground, fading)*
Line B: |E *direct*| (no ground reflection)

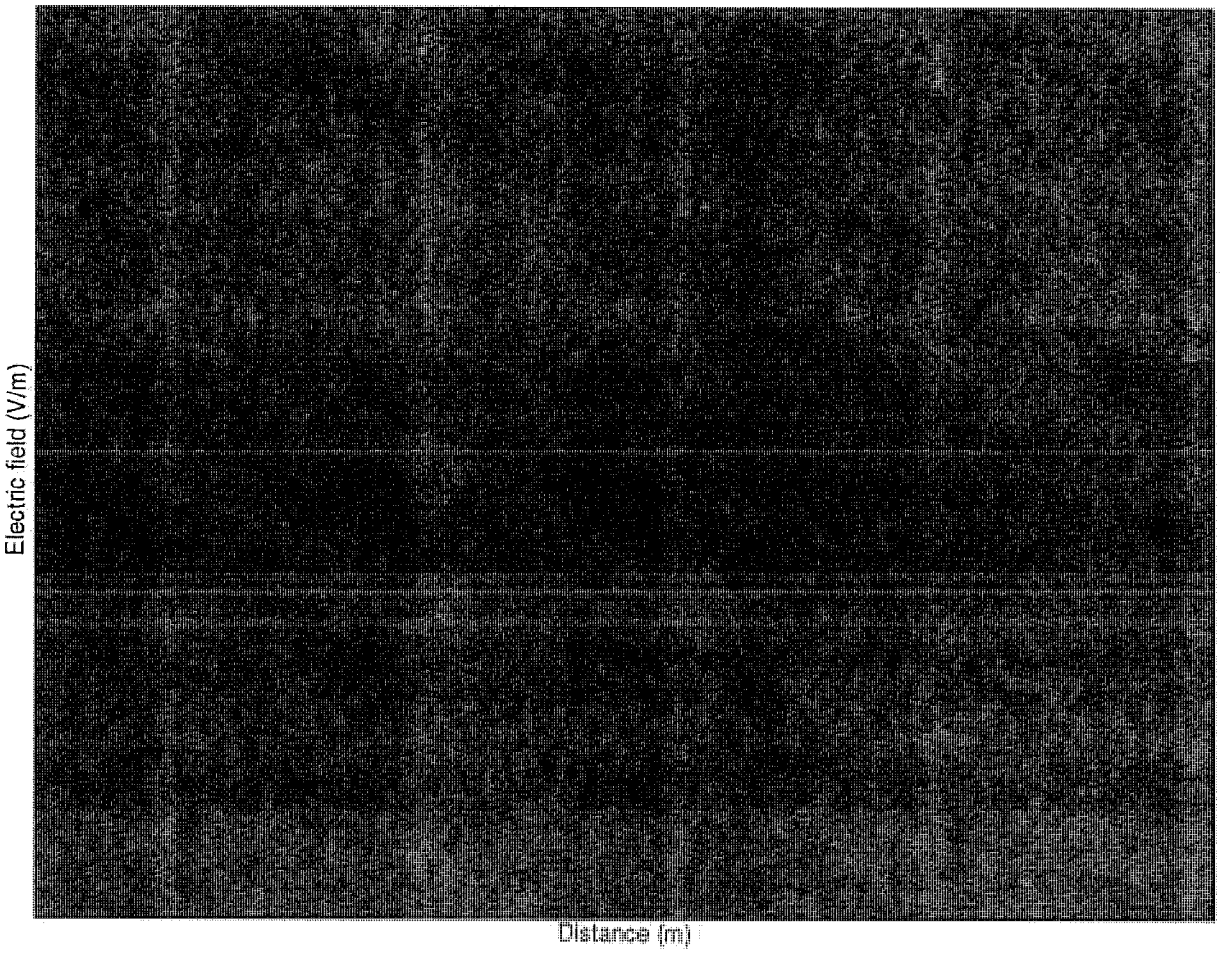

Figure 5.5: *(Same figure as Figure 5.4 but for a different range.)*
Theoretic electric field intensity E in point P(d,h) at distance d and height h while HIPIR is directed to point P(d,h). (constructive interference and perfect reflection assumed except for Line A).

Line 1:	E *direct*	+	E *reflected*	*at h = 0 m (perfectly conducting ground)*
Line 2:	E *direct*	+	E *reflected*	*at h = 0.5 m (perfectly conducting ground)*
Line 3:	E *direct*	+	E *reflected*	*at h = 1.0 m (perfectly conducting ground)*
Line 4:	E *direct*	+	E *reflected*	*at h = 1.5 m (perfectly conducting ground)*
Line 5:	E *direct*	+	E *reflected*	*at h = 1.9 m (perfectly conducting ground)*
Line A:	E *direct*	+	E *reflected*	*at h = 1.9 m (dry ground, fading)*
Line B:	E *direct*		(no ground reflection)	

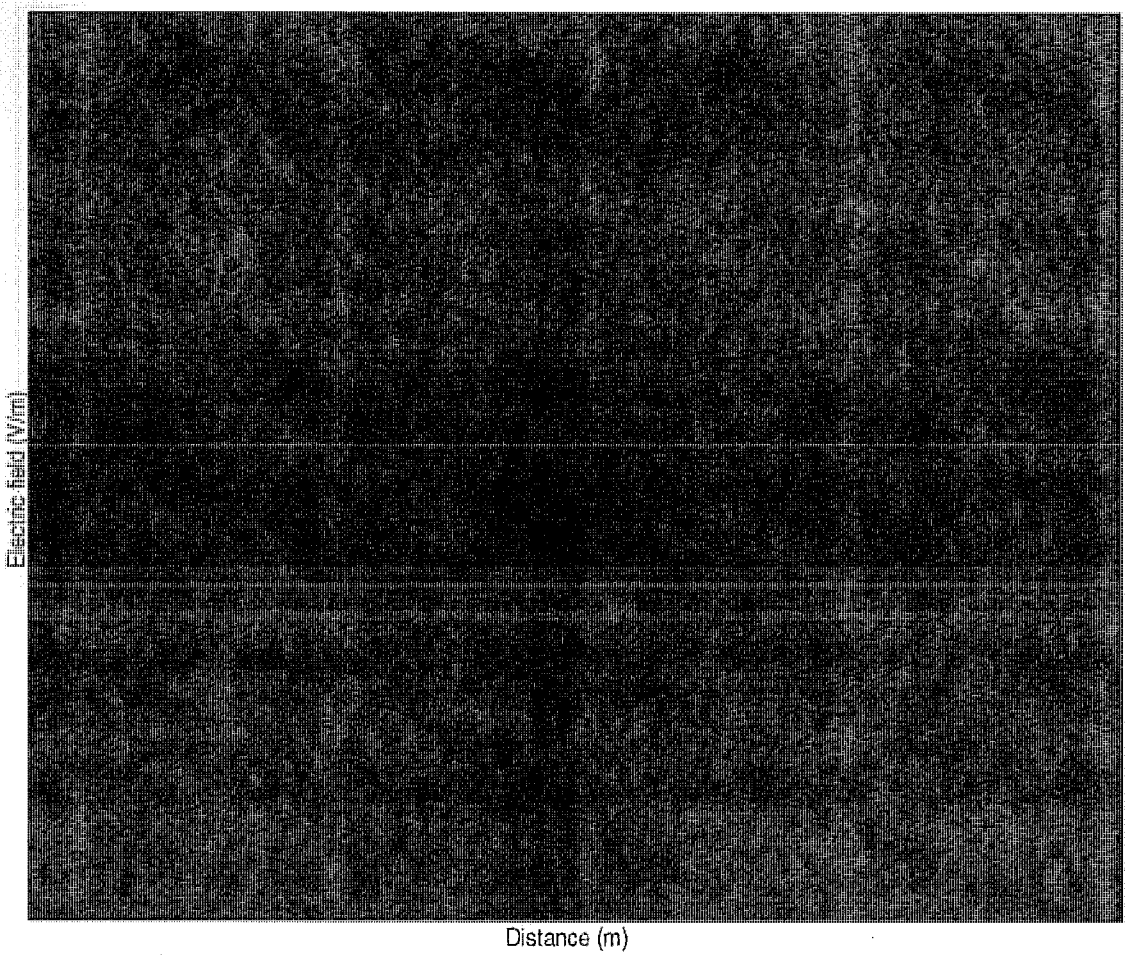

Figure 5.6: Theoretic electric field intensity E in point P(d,h) at distance d and height h, while HIPIR is directed to point Q(d,h=0). (Constructive interference and perfect reflection assumed).

Line 1: |E *direct*| + |E *reflected*| *at h=0 m (perfectly conducting ground)*
Line 2: |E *direct*| + |E *reflected*| *at h=0.5 m (perfectly conducting ground)*
Line 3: |E *direct*| + |E *reflected*| *at h=1.0 m (perfectly conducting ground)*
Line 4: |E *direct*| + |E *reflected*| *at h=1.5 m (perfectly conducting ground)*
Line 5: |E *direct*| + |E *reflected*| *at h=1.9 m (perfectly conducting ground)*
Line A: |E *direct*| (no ground reflection)

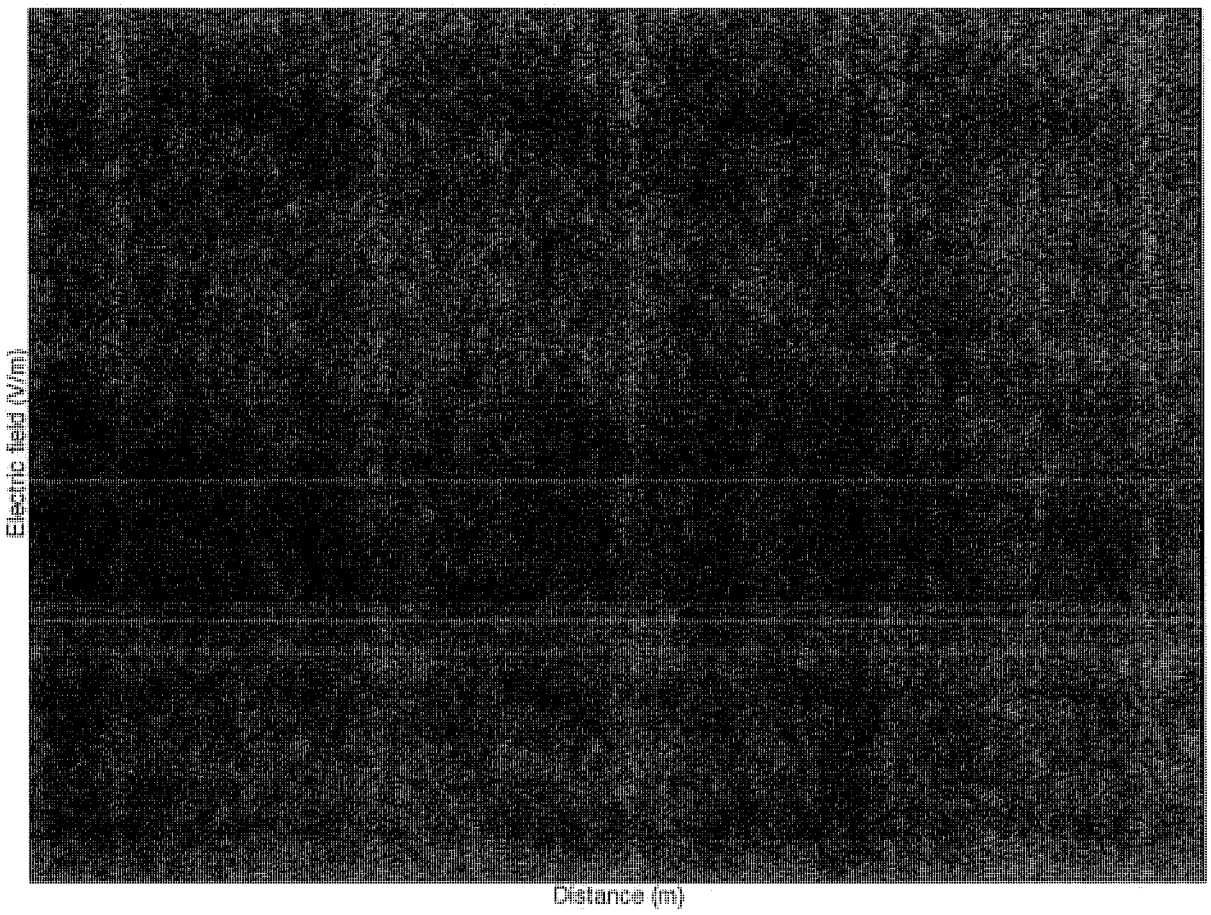

Figure 5.7 (Same figure as *Figure 5.6 but for a different range.)*

Theoretic electric field intensity E in point P(d,h) at distance d and height h, while HIPIR is directed to point Q(d,h=0). (Constructive interference and perfect reflection assumed).

Line 1: |E *direct*| + |E *reflected*| *at h=0 m (perfectly conducting ground)*
Line 2: |E *direct*| + |E *reflected*| *at h=0.5 m (perfectly conducting ground)*
Line 3: |E *direct*| + |E *reflected*| *at h=1.0 m (perfectly conducting ground)*
Line 4: |E *direct*| + |E *reflected*| *at h=1.5 m (perfectly conducting ground)*
Line 5: |E *direct*| + |E *reflected*| *at h=1.9 m (perfectly conducting ground)*
Line A: |E *direct*| (no ground reflection)

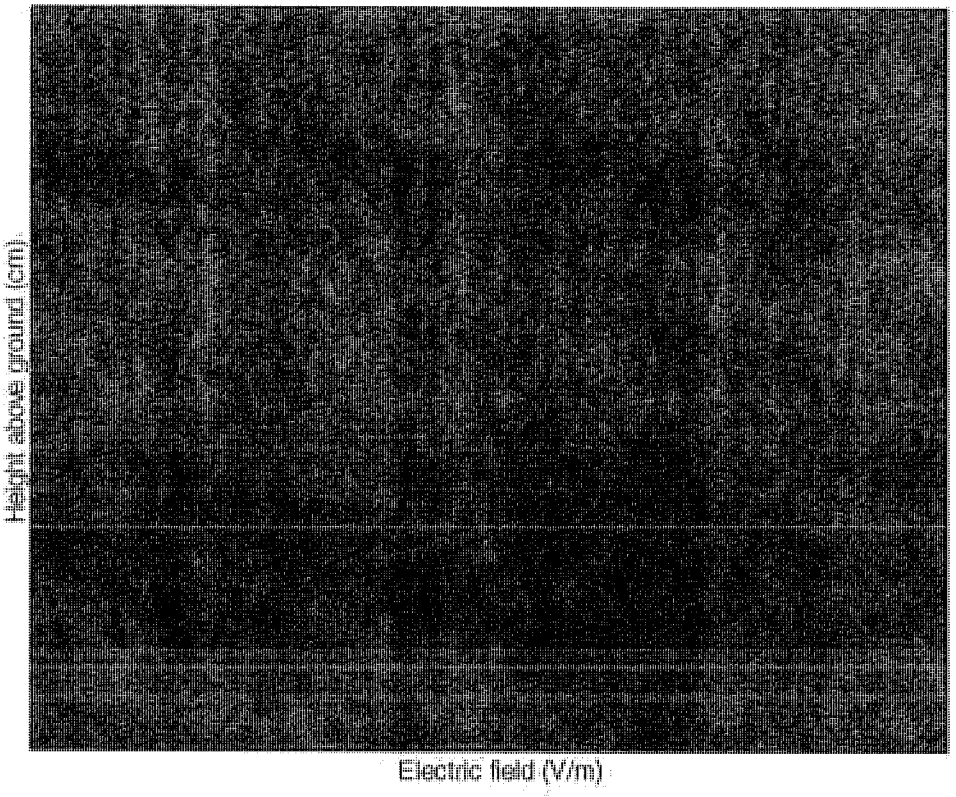

Figure 5.8: *Theoretic electric field intensity between h= 0 m and h=2 m height at* [redacted] *m distance from the HIPIR. (perfectly conducting, flat ground assumed)*

Line 1: |E *direct* + E *reflected*|, *for 0 m<h<2 m*
while HIPIR antenna pointed to Q(d=111.5 m, h=0 m)
($E_{rms\ with\ respect\ to\ height\ interval\ 0m\text{-}2m}$ = [redacted] *V/m)*

Line 2: |E *direct* + E *reflected*|, *for 0 m<h<2 m*
while HIPIR antenna pointed to Q(d=111.5 m, h=0.5 m)
($E_{rms\ with\ respect\ to\ height\ interval\ 0m\text{-}2m}$ = [redacted] *V/m)*

Line 3: |E *direct* + E *reflected*|, *for 0 m<h<2 m*
while HIPIR antenna pointed to Q(d=111.5 m, h=1.5 m)
($E_{rms\ with\ respect\ to\ height\ interval\ 0m\text{-}2m}$ = [redacted] *V/m)*

Line 4: |E *direct* + E *reflected*|, *for 0 m<h<2 m*
while HIPIR antenna pointed to Q(d=111.5 m ,h=1.9 m)
($E_{rms\ with\ respect\ to\ height\ interval\ 0m\text{-}2m}$ = [redacted] *V/m)*

Dashed lines represent the envelopes of lines 1, 2, 3 and 4.

5.2 CWAR theoretical results

5.2.1 Basic assumptions

The beam-width of the CWAR antenna and its dimensions indicate, using the criteria of Appendix D, that the illumination in the antenna aperture can be regarded as a $\cos^3$ shaped field distribution in the vertical direction and a uniform distribution in the horizontal direction. To estimate the electric field strength, calculations have been made assuming the specifications of Section 3.3.2.

5.2.2 Calculations for non-rotating CWAR antenna

The electric field intensity was calculated for field points at distances between 5 m and 1000 m from the CWAR at heights of 2.77 m (main-beam), 1.9 m, 1.5 m and 0.5 m, assuming the CWAR's elevation angle set to 0 degrees (Figure 5.9). The results are presented in Figure 5.10 and Figure 5.11 for respectively no ground reflection and perfect ground reflection. In case of the reflecting ground, calculations were made using an additional virtual mirror source whereas the absolute values of direct and reflected waves were added as shown in Figure 4.3 (constructive interference). Comparing Figure 5.10 and Figure 5.11 shows that at distances smaller than 40 m from the CWAR the reflection doesn't play a significant role. In the Fresnel region the maximum field intensity within the main-beam doesn't necessarily occur at an azimuth angle of 0 degrees as shown by Figure 5.13 and Figure 5.14.
In Figure 5.13 the normalised field intensity is displayed for different distances and azimuth angles. The beam-width becomes smaller for increasing distances until the far-field distance is reached. Figure 5.14 shows an electric field intensity contour plot.

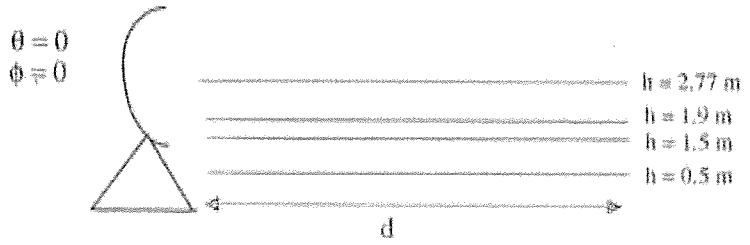

Figure 5.9: CWAR calculations at heights h=2.77 m, 1.9 m, 1.5 m and 0.5 m.

5.2.3 Calculations for rotating CWAR antenna

If the CWAR antenna is rotating, the root of the mean square electric field intensity (E_{rms}) over the azimuth range of 360 degrees has to be determined. In Figure 5.12 the electric field intensity correction factor for a rotating CWAR antenna is presented. The electric field within the main-beam has to be multiplied by this factor to obtain the average field intensity at main-beam height (2.77 m) generated

by a rotating antenna. If this value is raised to the square and divided by 377Ω, the average power density in W/m^2 is obtained.

5.2.4 Conclusion theoretical results CWAR

Approaching the non-rotating CWAR at a height of h = 1.9 m the electric field nowhere exceeds the STANAG 2345 (edition-2, 1997) whole body continuous exposure level of 194 V/m (Figure 5.10 and Figure 5.11). At a height of 2.77 m, using Figure 5.14 to determine electric field intensities at different azimuth angles, it can be shown that within [redacted] m from the non-rotating CWAR antenna the 194 V/m limit is exceeded. For a rotating CWAR the average exposure will be smaller than for a non-rotating radar.

5.3 IFF calculations

Using the specifications of Section 3.4.2 electric fields can be calculated by using the far-field expression of the electric field (see Equation (5-1)). Near the IFF antenna this equation can be used to determine an upper limit of the electric field intensity for a non rotating antenna. Calculations show that at distances of [redacted] m or more the average power density will be smaller than [redacted] W/m^2 which corresponds to an electric field intensity of [redacted] V/m. Assuming perfect ground reflection the upper electric field bound will be doubled to become [redacted] V/m.
So at a distance of more than 3 m from the IFF antenna the electric field will be smaller than the STANAG 2345 (edition-2, 1997) whole body continuous exposure limit of 112 V/m (at 1 GHz).

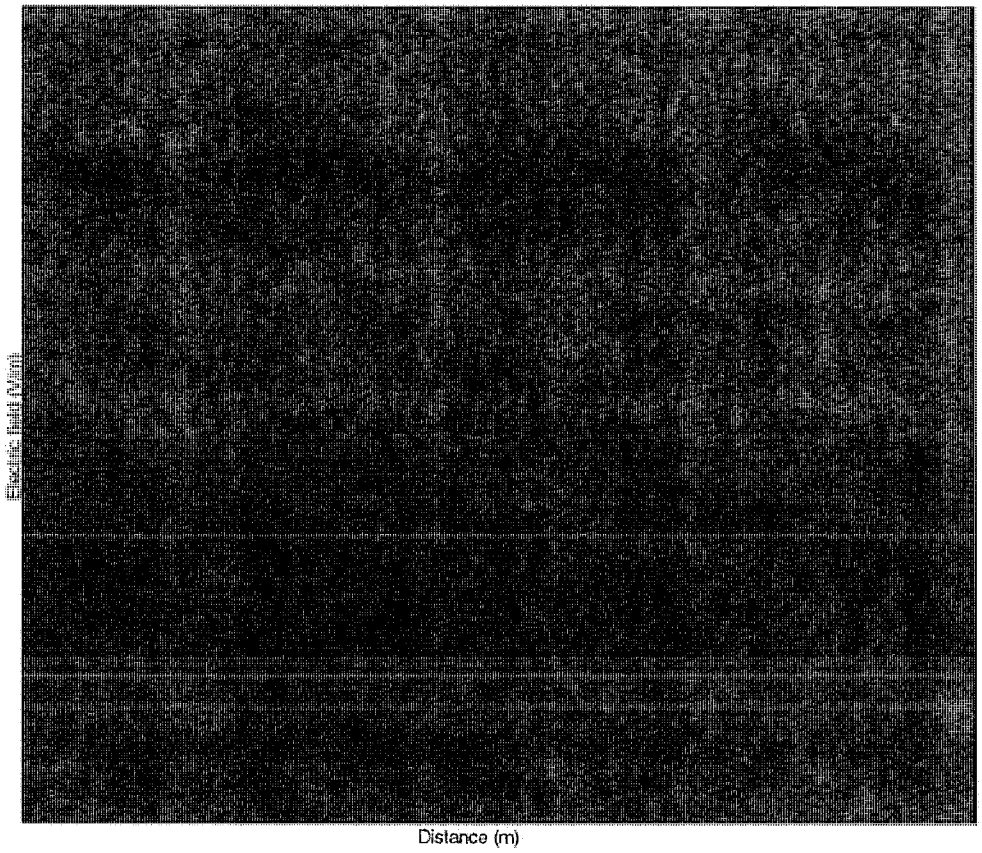

Figure 5.10: Electric field intensity at different heights below CWAR's main-beam without ground reflection. Line 1: h = 2.77 m (in main-beam), Line 2: h = 1.9 m; Line 3: h = 1.5 m; Line 4: h = 0.5 m.

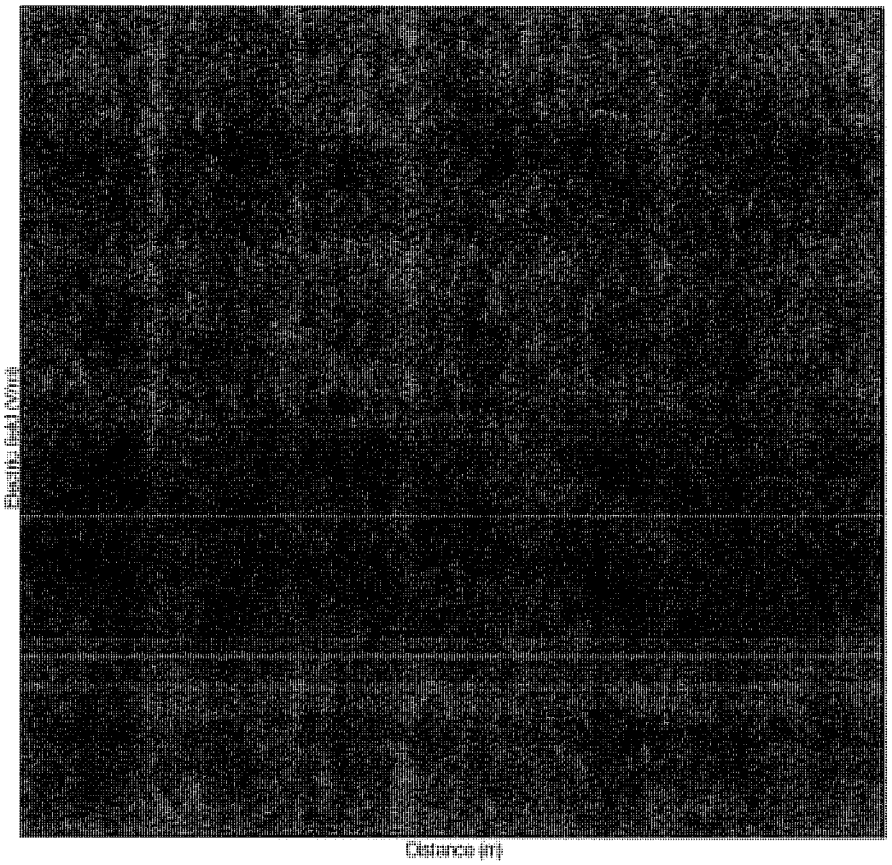

Figure 5.11: Electric field intensity in and at different heights below CWAR's main-beam with maximum ground reflection. Line 1: h = 2.77 m (in main-beam), Line 2: h = 1.9 m; Line 3: h = 1.5 m; Line 4: h = 0.5 m.

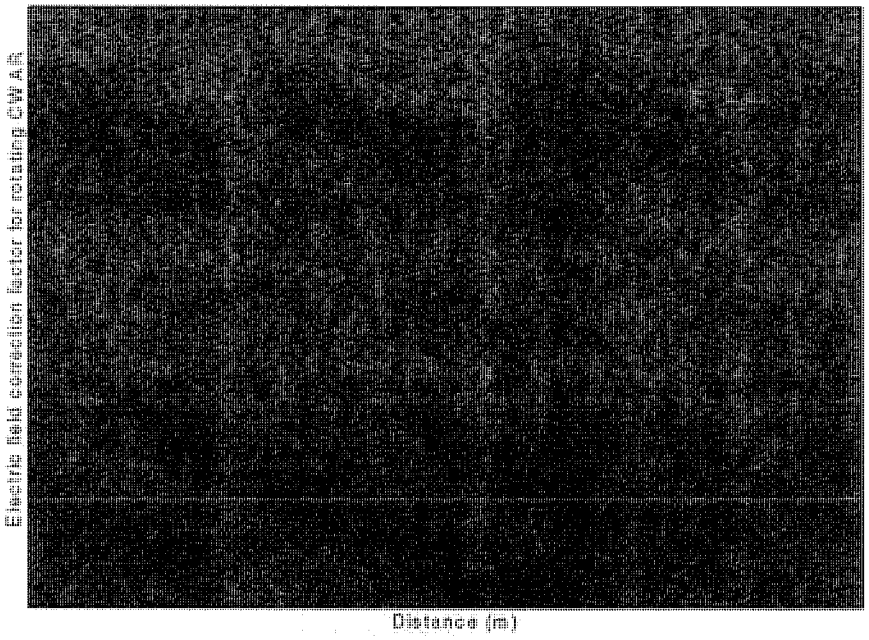

Figure 5.12: *Electric field intensity weighting factor for rotating CWAR. The electric field within the main-beam has to be multiplied by this factor to obtain the average electric field intensity at main-beam height (h=2.77 m).*

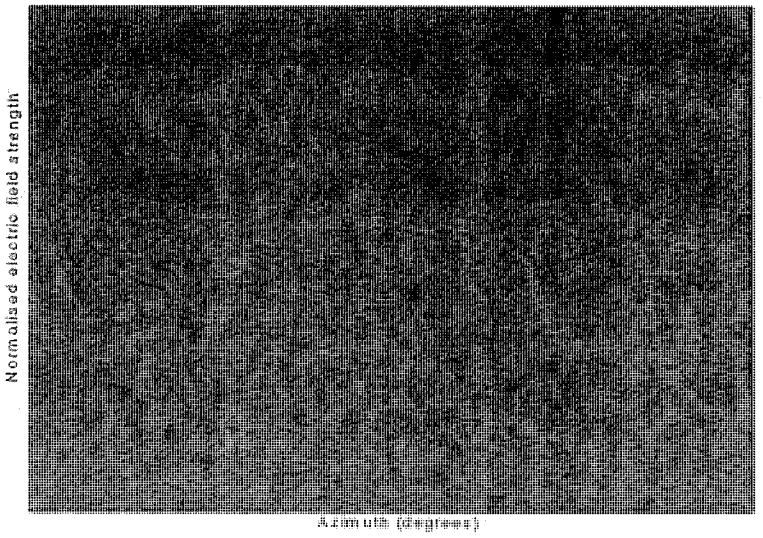

Figure 5.13: *Normalised electric field intensity as a function of azimuth angle for CWAR at different distances. dark blue: 20 m, light blue: 50 m, purple: 100 m, light brown: 1000 m.*

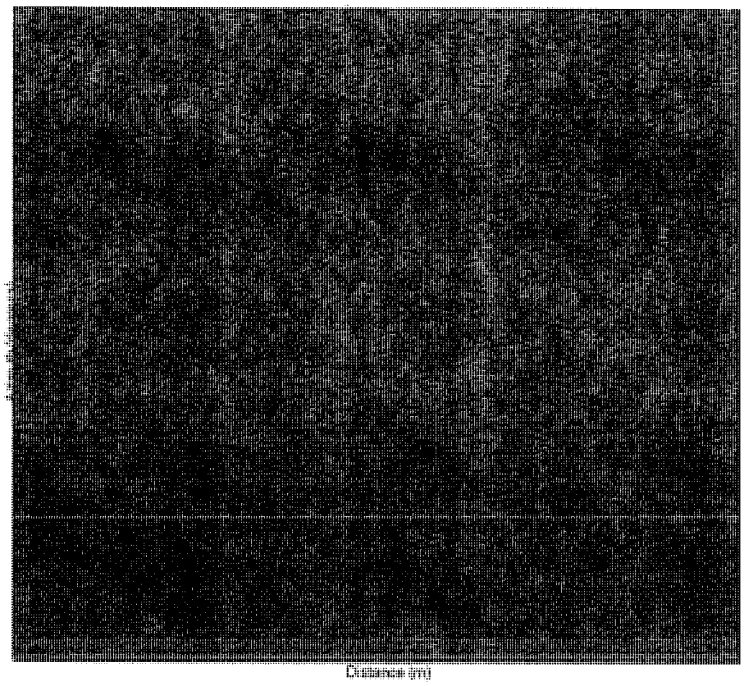

Figure 5.14: Contour plot of electric field intensity generated by CWAR at height $h = 2.77$ m.
Although calculations are based on no ground reflections, results can be used for a situation with ground reflections because till approximately 40 m ground reflections can be neglected.

[redacted]

6. Measurements

In order to get a complete picture of the electromagnetic field intensity near the HAWK installation, the electric fields were measured in an environment where reflecting objects were removed as well in a real environment where the radars were pointed to different locations inside the Twenthe Air Base HAWK installation.

6.1 Measurement equipment and software

To measure the electric field intensity generated by the different HAWK sources, two isotropic field probes were used:

HI-95440 serial number 95440, RF electric field probe 1 V/m - 300 V/m
HI-4456 serial number 97982, RF electric field probe 30 V/m - 1000 V/m

They were mounted on a wooden tripod at fixed heights of 1.5 m and 1.9 m. Via a glass fiber cable the measurement data was transported from the probes to a laptop controller installed in the PCP. Software was developed to collect and archive the measurement data (Figure 6.1). For each measurement position and for each probe, 30 measurements with intervals of 1 s were recorded during 30 s and the time averaged value was calculated.

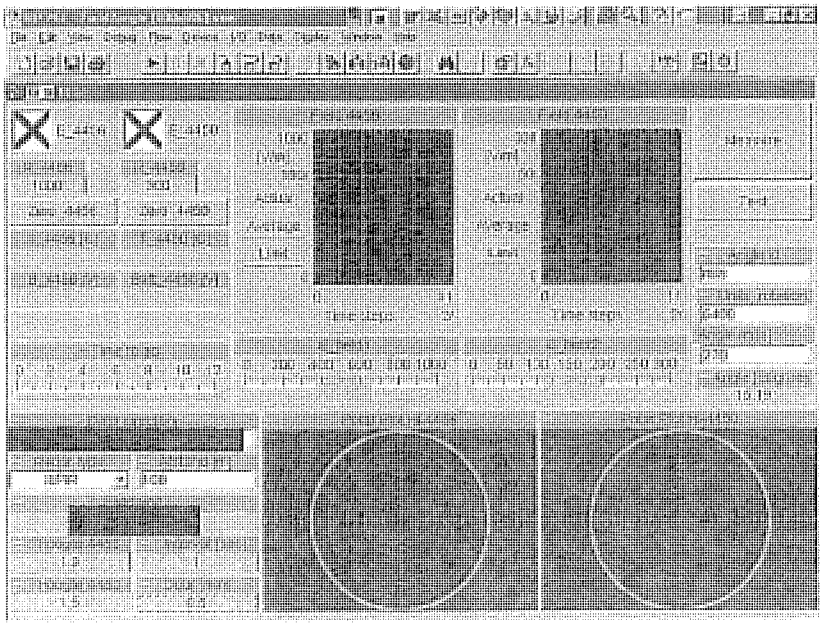

Figure 6.1: Screen dump of control and acquisition software.

Prior to taking measurements, both field probes were validated at the NLR (National Aerospace Laboratory) in a fully anechoic chamber for the frequency of 10 GHz. During this validation the probe orientations for maximum sensitivity for vertical polarisation were recorded. To prevent non isotropicity effects during the HAWK measurements, the probes always were orientated in these positions of maximum sensitivity for vertical polarisation (even for CWAR measurements for which horizontal polarisation applies). Using calibration reports and the validation information, the probe correction factors were obtained for vertical and horizontal polarisation. Raw measurement data had to be multiplied by these factors to obtain the electric field intensity in V/m. Because the amount of measurement data was too large to include in this report, the complete set of measurement results have been filed in the project archive conform standard TNO procedures.

6.2 Individual radar measurements

To obtain information on electric fields generated by the HIPIR and the CWAR, electric field measurements were conducted at fixed heights of 1.5 m and 1.9 m at various distances. Preceding these measurements, obstacles were removed out of the radar's main-beam to prevent object reflections. During the measurements the elevation of the CWAR antenna was maintained at 0 degrees (Figure 6.2) whereas the elevation of the HIPIR was adjusted for maximum reading of the upper field probe (Figure 6.3). For both radars azimuth radiation patterns were obtained by rotating the radar antenna in discrete steps maintaining the probes in fixed positions. Figure 6.4 gives an impression of the measurement installation for CWAR and HIPIR with the measuring distances.

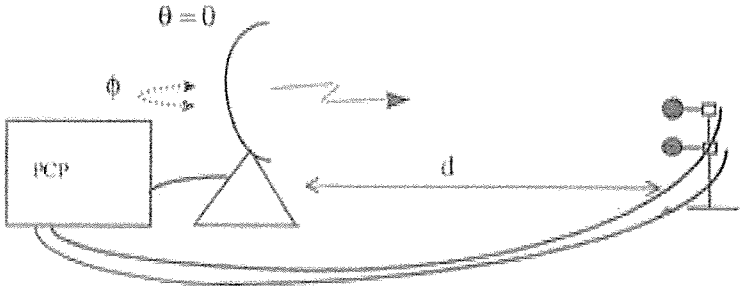

Figure 6.2: Measurement installation for CWAR and HIPIR (elevation = 0 degrees)

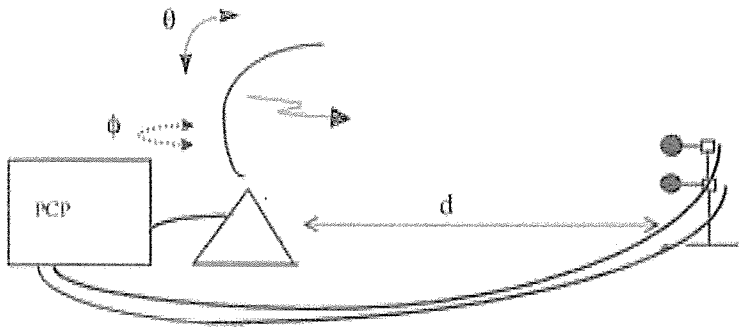

Figure 6.3: Measurement installation for HIPIR, (elevation adjusted for maximum reading of the upper probe (1.9 m)

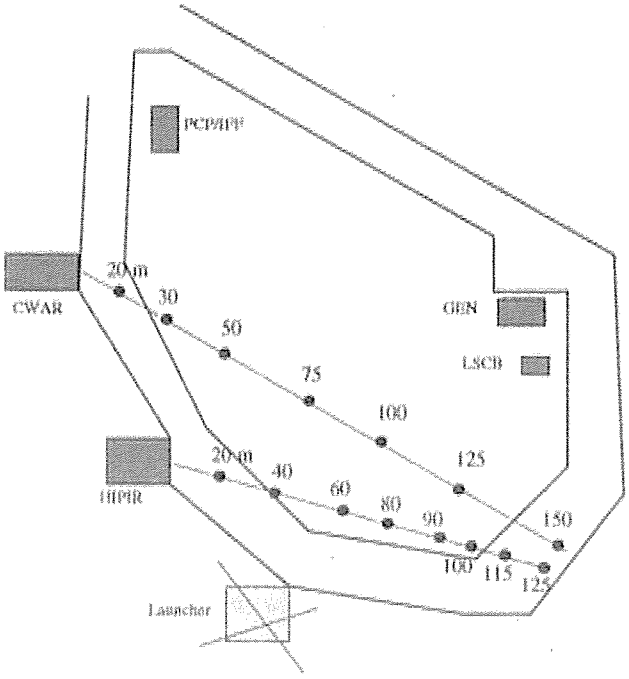

Figure 6.4: Impression of measurement installation for CWAR and HIPIR (not on scale), view from above. The launcher was removed to prevent reflections, whereas the probes were positioned at several locations along the dashed lines.

6.3 HAWK installation measurements

Supplementary to the electric field measurements of the individual radars in an environment without reflecting objects, measurements have been conducted at several accessible locations (Figure 6.5) within the real HAWK installation boundary at Twente Air Base.

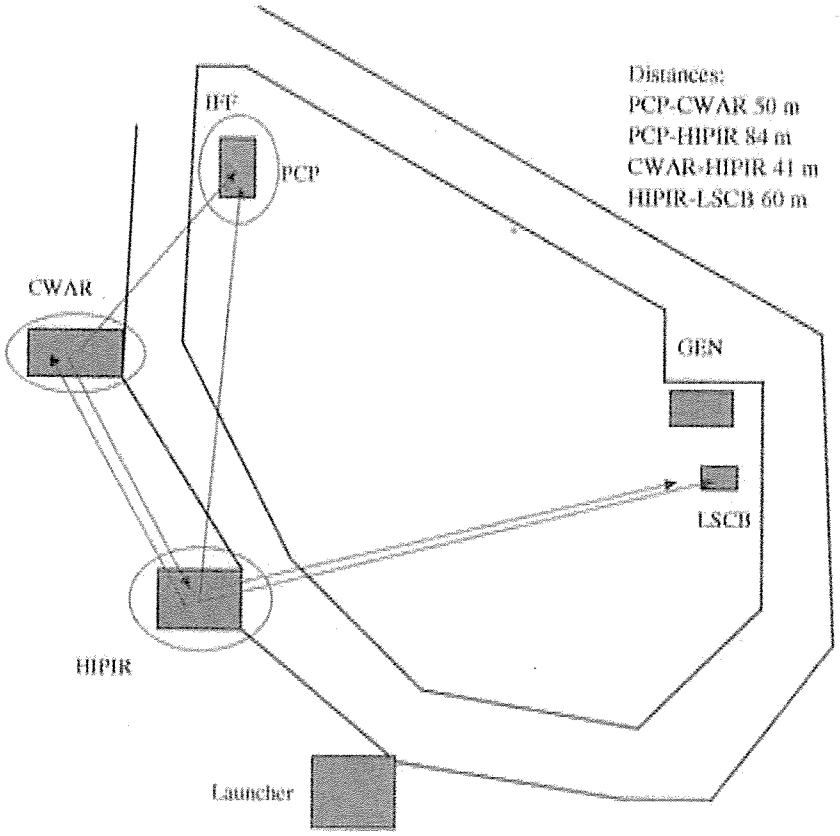

Figure 6.5: Measurements within the HAWK installation boundary at Twenthe Air Base (not on scale).

Measurements have been performed at the following locations:

- Probes on top of PCP, radiated by CWAR.
- Probes on top of HIPIR, radiated by CWAR.
- Around CWAR while CWAR is radiating.
- Probes on top of PCP, radiated by HIPIR.
- Probes in PCP, radiated by HIPIR.
- Probes on top of HIPIR behind antenna, while HIPIR is radiating.
- Around HIPIR while HIPIR is radiating.
- Probes inside and outside LSCB, radiated by HIPIR.

6.4 Measurement results

6.4.1 HIPIR measurement results

Measurements were performed as described in Section 6.2. Because of the large amount of measurement data, the complete set of measurement results have been filed in TNO archives. Results obtained for the situation where the HIPIR was adjusted for maximum reading of the upper field probe (height h = 1.9 m) are plotted in Figure 6.6. Measurement results at h = 1.9 m are in good agreement with theory and fluctuate around the theoretical bound corresponding to that height (line 5). At some locations, the theoretical h = 1.9 m bound is exceeded, which can be explained by height differences of the terrain; a relatively small deviation from h = 1.9 m can have a major impact on the field intensity as shown in the plots.

Additional measurements were conducted at the following locations:

a) On top of PCP, radiated by HIPIR: [redacted] V/m (84 m).
b) In PCP, radiated by HIPIR: [redacted] V/m (84 m).
c) On top of HIPIR, behind antenna while radiating: [redacted] V/m.
d) Around HIPIR while HIPIR is radiating:
   - at h = 1.9 m directly under antenna: [redacted] V/m,
   - beside and behind the HIPIR: E[redacted] V/m,
e) Inside and outside LSCB, radiated by HIPIR (60 m):
   - in front of LSCB: [redacted] V/m,
   - in LSCB behind window: [redacted] V/m,
   - in centre of LSCB: [redacted] V/m.

At the locations (radiated by HIPIR) on top of the PCP, in front of LSCB and in the LSCB behind the window, the STANAG 2345 (edition-2, 1997) limit is exceeded.

Generally if reflecting objects are in the vicinity of a measurement point, the measured electric field intensity can exceed the expected value that arise for only ground reflection.

Figure 6.6: *Measured (o) and theoretic electric field intensity E in point P(d,h) at distance d and height h*
solid lines: *HIPIR antenna pointed to Q(d,h)=P(d,h), (theoretic situation 1, see Section 5.1.3)*
dashed lines: *HIPIR antenna pointed to Q(d,h=0), (theoretic situation 2, see Section 5.1.3)*
o: *Measured electric field intensity at h=1.9 m.*

Green: |E *direct*| + |E *reflected*| *at h=0 m, perfectly conducting ground,*
Black: |E *direct*| + |E *reflected*| *at h=0.5 m, perfectly conducting ground,*
Mag: |E *direct*| + |E *reflected*| *at h=1.0 m, perfectly conducting ground,*
Blue: |E *direct*| + |E *reflected*| *at h=1.5 m, perfectly conducting ground,*
Red: |E *direct*| + |E *reflected*| *at h=1.9 m, perfectly conducting ground,*
Yellow: |E *direct*|, no ground reflections.

6.4.2 CWAR measurement results

Measurements were performed as described in Section 6.2. Because of the large amount of measurement data, the complete set of measurement results have been entered in a separate document named: 'Hawk measurement results'. Some results are displayed in Figure 6.7 (with theoretical no-reflection curves) and Figure 6.8 (with theoretical maximum reflection curves). As expected the results show that the measured values are below the theoretical maximum values for 1.9 m and 1.5 m. The reason that some measured values are significantly below the theoretical maximum possible values can be found in:

- Direct and reflected components do not add in phase.
- Differences in terrain height.
- Power P and/or antenna gain G specified by the manufacturer deviate from reality.
- CWAR elevation angle > 0 degrees.
- Measurement errors (see Appendix E).

Additional measurements were performed at the following locations:

a) On top of PCP radiated by CWAR: [redacted] V/m;
b) On top of HIPIR radiated by CWAR: [redacted] V/m ;
c) Around CWAR while CWAR is radiating: [redacted] V/m.

Generally if reflecting objects are in the vicinity of a measurement point, the measured electric field intensity can exceed the expected value that arise for only ground reflection.

Figure 6.7: *CWAR E field measurement at h = 1.9 m (o) and h = 1.5 m (*). Theoretical electric field in (h=2.77 m) and at different heights below CWAR's main-beam without ground reflection.*

dashed blue: *h = 2.77 m (no near-field correction see Eq.(4.1)),*
blue: *h = 2.77 m (in main-beam),*
green: *h = 1.9 m,*
red: *h = 1.5 m,*
light blue: *h = 0.5 m.*

Figure 6.8: *CWAR E field measurement at h = 1.9 m (o) and h = 1.5 m (*)*
Theoretical electric field in and at different heights below CWAR's main-beam with ground reflection (constructive interference).
blue: *h = 2.77 m (in main-beam),*
green: *h = 1.9 m,*
red: *h = 1.5 m,*
light blue: *h = 0.5 m.*

6.4.3 IFF measurement results

The electric field generated by the IFF antenna was measured around the PCP at a height of 1.9 m above the ground. The IFF antenna was installed on top of the PCP. Because the IFF antenna transmits pulses, the HI-4456 thermal isotropic electric field probe, designed to measure pulse shaped field variations, was used to determine the electric field intensity. The field sensor did not respond which means that the electric field intensity value was smaller than 30 V/m (lowest value in probe range).

[redacted]

7. Conclusion

To determine the electric field intensity near the HAWK installation, in December 1998 measurements have been performed on the CWAR and the HIPIR radars, which are part of the HAWK installation at Twenthe Air Base. To support the measurements and to be able to inter- and extrapolate the results a theoretical analysis was made. The theoretical predictions turned out to be in good conformity with the measurement results. Both measurement and theoretical results were compared to STANAG 2345 (edition-2, 1997) exposure limits.

7.1 HIPIR

From the theoretical results and the measurement data it follows that the electric field intensity at any point depends on the distance from that point to the HIPIR, the height of that point above the ground and the elevation angle of the HIPIR antenna. At the moment the HIPIR safety distance as used by the Royal Netherlands Airforce amounts 111.5 m. From the theoretical results it follows that at this distance, in a worst case situation, assuming a perfectly flat reflecting ground, constructive interference and a negative antenna elevation angle, the electric field intensity locally can have values of maximal [redacted] V/m for heights lower than or equal to 1.9 m. Because of fading (fluctuations in field strength as a function of the height above ground), the average electric field intensity (in the height interval from ground level to 2 m) will be smaller and amounts [redacted] V/m. According to STANAG 2345 (edition-2, 1997) these values indicate that at 111.5 m from the HIPIR, continuous whole body and partial body (except for the eyes) exposure is permitted. Purely based on HIPIR measurements, performed at distances larger than or equal to 111.5 m at heights of 1.5 m and 1.9 m at Twenthe Air Base, the restriction for the eyes strictly does not apply.
Some additional HIPIR measurements were conducted at several locations within the HAWK site. Locations were the STANAG (edition-2, 1997) whole body continuous exposure limit was exceeded in case of directing the beam to it, were:

a) On top of the PCP, radiated by HIPIR: [redacted] V/m (84 m from the HIPIR antenna).
b) Inside and outside the LSCB, radiated by HIPIR:
   - in front of the LSCB: [redacted] V/m, (60 m from HIPIR antenna),
   - inside the LSCB behind window: [redacted] V/m (60 m from the HIPIR antenna).

At all of these locations the distance to the HIPIR is smaller than the safety distance of 111.5 m.

7.2 CWAR

Both the theoretical analysis and the measurements results show that for heights lower than or equal to 1.9 m the electric field intensities, at any distance from the rotating or non-rotating CWAR antenna (with non negative elevation angle), are below the STANAG 2345 (edition-2, 1997) whole body continuous exposure limit of 194 V/m.
So according to STANAG 2345 (edition-2, 1997) for heights equal to or smaller than 1.9 m, continuous whole body exposure is permitted at any distance from the CWAR.
No measurements were performed within the main-beam. Theoretical analysis shows however that the 194 V/m level can be reached at [redacted] m distance from the non-rotating CWAR at a height of 2.77 m (height of centre of the antenna). The average exposure becomes smaller if the CWAR antenna is rotating.
At the moment, the safety distance at antenna height (2.77 m) as used by the Royal Netherlands Airforce, amounts 74 m for a non-rotating CWAR antenna. In the past this distance was 45 m. Both values are larger than [redacted] m. So according to STANAG 2345 (edition-2, 1997) at the formerly used safety distance of 45 m as well as at the currently used safety distance of 74 m, continuous whole body exposure is permitted.

8. References

[1] TM 9-1425-152 HAWK Technical Manual

[2] ANSI C95.3-1973 American National Standard Techniques and Instrumentation for the Measurement of Potentially Hazardous Electromagnetic Radiation at Microwave Frequencies.

[3] Microwave antenna theory and design
Boston Technical Publishers, inc. Samual Silver

[4] Vermogensdichtheden in de Fresnel-zone
Physisch Laboratorium TNO; [redacted]
Rapportnummer IR 1974-68

[5] The scattering of electromagnetic waves from rough surfaces
[redacted]
Pergamon Press 1963

[6] ITU Recommendations 527-3

[7] College diktaat: Antennes en propagatie
TU Eindhoven; [redacted]

[8] Collegediktaat Radio en Radar
TU Eindhoven; [redacted]

[redacted]

9. Signature

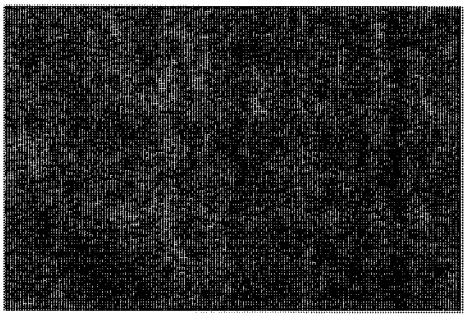

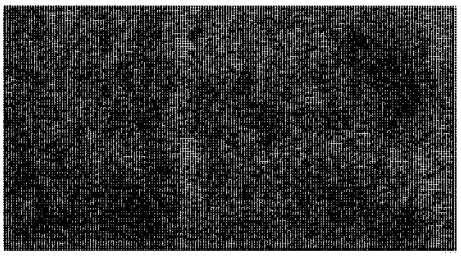

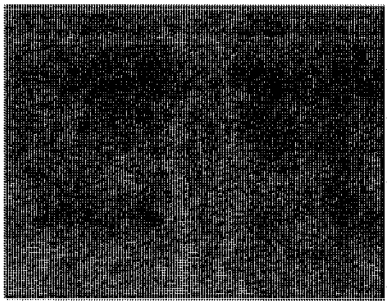

[redacted]

Appendix A Field calculation

Electric fields generated by aperture antennas (Figure A.1) can be calculated using the equivalence principle which states that actual three dimensional sources, (antenna and transmitter in region 1), can be replaced by fictitious equivalent sources in a two dimensional area (the opening of the antenna named aperture) if the tangential field distribution in that area is known. Just outside, in front of the aperture, the generated waves are assumed to be plane waves with equal phase and polarisation. Outside the aperure, the fields in the plane of the aperture, are assumed to be zero.

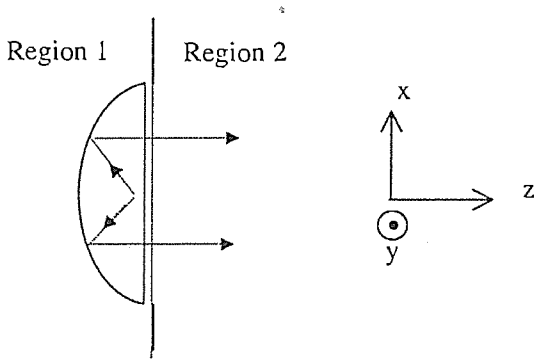

Figure A.1: Side view of antenna aperture (vertical dashed line)

Knowing the field distribution in the plane of the aperture, the generated fields in Region 2 $\overline{E_2}$ and $\overline{H_2}$ can be thought to be generated by equivalent electric and magnetic surface current density sources in the aperture:

$$\overline{K}_e = -\overline{n} \times \overline{H_1} \,, \tag{A.1}$$

$$\overline{K}_m = \overline{n} \times \overline{E_1} \,, \tag{A.2}$$

in which:

$\overline{K_e}$: Electric surface current density [A/m];
$\overline{K_m}$: Magnetic surface current density [V/m];
$\overline{H_1}$: Tangential magnetic field in aperture [A/m];
$\overline{E_1}$: Tangential electric field in aperture [V/m];
$\overline{n}$: Unit vector normal to aperture surface directed to Region 1.

These currents, flowing through small surface elements can be associated with currents flowing through infinitesimal small electric and magnetic dipoles.

For $\overline{E_1}$ pointing in the -x direction these dipole currents become:

$$\overline{I_e} = \left[\frac{\left|\overline{E_1}\right|}{Z_0} dy\right] \overline{e_x} \quad . \tag{A.3}$$

$$\overline{I_m} = \left[\left|\overline{E_1}\right| dx\right] \overline{e_y} \quad . \tag{A.4}$$

in which:

$\overline{I_e}$ denotes the electric dipole current [A],
$\overline{I_m}$ denotes the magnetic dipole current [V].

Using the relations for fields generated by infinitely small electric and magnetic dipoles (not given here), it can be shown that an individual surface element *dxdy* (for $\overline{E_1}$ directed in positive x direction) generates an electric field [8] equal to:

$$dE_\theta = (dE_\theta)_e + (dE_\theta)_m = -B\cos(\phi')\,(\cos(\theta')+1)\,, \tag{A.5}$$

$$dE_\phi = (dE_\phi)_e + (dE_\phi)_m = +B\sin\phi'(1+\cos(\theta'))\,, \tag{A.6}$$

in which B is given by:

$$B = \frac{j\,E_1\,dxdy}{2\lambda\,R'}\,e^{j(\omega t-\beta R')} \tag{A.7}$$

The total field generated in point P(x,y,z) due to sources in an aperture A (Figure A.2), with field distribution $E_1 = E_1(\eta,\xi)$ in the aperture, can be expressed by:

$$\overline{E}(x,y,z) = \iint_A \frac{jE_1(\eta,\xi)}{2\lambda R'}\cdot\left(1+\cos\theta'\right)\cdot$$

$$\left[\overline{e_{\theta'}}\left(-\cos\phi'\right)+\overline{e_{\phi'}}\left(\sin\phi'\right)\right]\cdot e^{-j\beta R'}\,d\eta d \tag{A.8}$$

in which

$R' = R'(\eta, \xi, x, y, z)$:	Distance from aperture point $Q(\eta,\xi)$ to P(x,y,z) [m],
$\theta' = \theta'(\eta, \xi, x, y, z)$:	Angle between z axis and vector from $Q(\eta,\xi)$ to P(x,y,z) [rad],
$\phi' = \phi'(\eta, \xi, x, y, z)$:	Angle between the line from P'(x,y,0) to $Q(\eta,\xi)$ and x axis [rad],

$\theta = \theta(\eta, \xi, x, y, z)$:	Angle between z axis and vector from Q(0,0) to P(x,y,z) [rad],
$\phi = \phi(\eta, \xi, x, y, z)$:	Angle between the line from P'(x,y,0) to Q(0,0) and x axis [rad],
$\beta = 2\pi/\lambda$:	[rad/m],
$E_1(\eta, \xi)$:	Electric field distributions in aperture A (E_1 vector oriented in positive x direction) [V/m]
P(x,y,z):	Point at which the field is calculated.
P'(x,y,z):	Projection of P on xy plane
$Q(\eta,\xi)$:	Point in aperture A (in xy plane)
$\overline{e_{\theta'}}$	Unit vector in θ' direction,
$\overline{e_{\theta}}$	Unit vector in θ direction,
$\overline{e_{\phi'}}$	Unit vector in ϕ' direction,
$\overline{e_{\phi}}$	Unit vector in ϕ direction.

At distances for which $\overline{e_{\theta'}} \approx \overline{e_{\theta}}$ and $\overline{e_{\phi'}} \approx \overline{e_{\phi}}$ Equation (A.8) can be approximated by

$$\left|\overline{E}(x,y,z)\right| \approx \left|\iint_A \frac{jE_1(\eta,\xi)}{2\lambda R'} \cdot (1+\cos\theta') \cdot e^{-j\beta R'} d\eta d\xi\right| \qquad \text{(A.9)}$$

to obtain the amplitude (also denoted as the intensity) of the electric field.

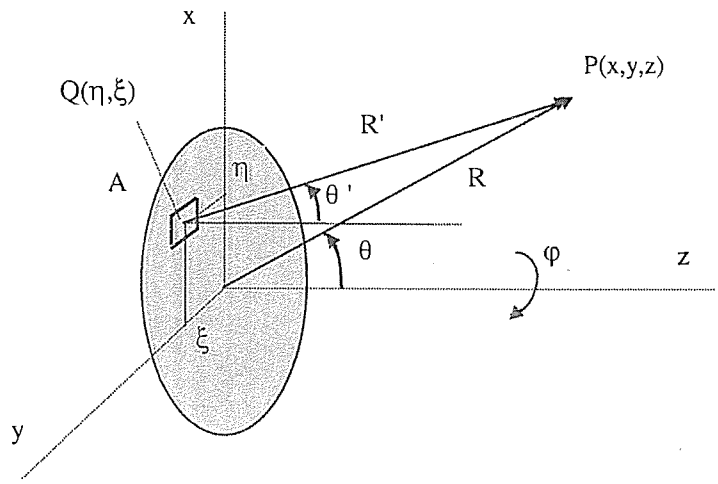

Figure A.2: Aperture geometry

Appendix B Reflection on plane boundaries

The reflection coefficient depends on the electrical parameters of the surface, the grazing angle and the direction of the electric field vector in relation to the plane of incidence. The plane of incidence is defined as the plane defined by the vector of propagation and the normal on the reflecting surface.
If the electric field vector $\overline{E}$ lies in the plane of incidence (Figure B.1) the reflection coefficient for a smooth surface can be expressed by [7]

$$\rho_{//} = \frac{n^2 \sin\psi - \sqrt{n^2 - \cos^2\psi}}{n^2 \sin\psi + \sqrt{n^2 - \cos^2\psi}} \quad . \tag{B.1}$$

The reflection coefficient for $\overline{E}$ perpendicular on the plane of incidence is given by:

$$\rho_{\perp} = \frac{\sin\psi - \sqrt{n^2 - \cos^2\psi}}{\sin\psi + \sqrt{n^2 - \cos^2\psi}}, \tag{B.2}$$

in which n^2 follows from

$$n^2 = \varepsilon_{r2} - j\frac{\sigma_2}{\omega\varepsilon_0}, \tag{B.3}$$

$\rho_{//}$: Reflection coefficient for E vector parallel to plane of incidence,
$\rho_{\perp}$: Reflection coefficient for E vector perpendicular to plane of incidence,
ψ: Grazing angle (angle between ground surface and the wave propagation direction)[rad],
σ_2: Conductivity ground [S/m],
ε_0: Permittivity vacuum [F/m],
ε_2: Permittivity of ground. [F/m],
n: Complex index of refraction.

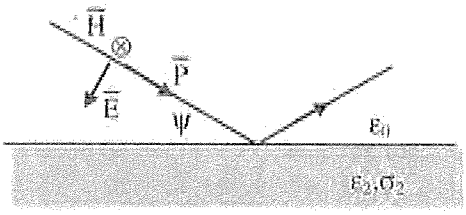

Figure B.1: Incident wave reflected on plane ground surface ($\overline{E}$ vector in plane of incidence). $\overline{P}$ denotes the Poynting vector.

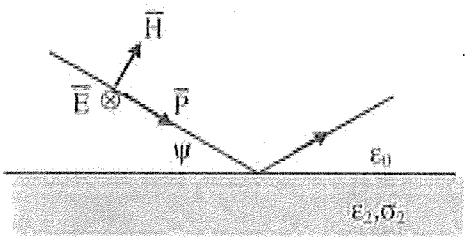

Figure B.2: Incident wave reflected on plane ground surface ($\overline{E}$ vector perpendicular on plane of incidence). $\overline{P}$ denotes the Poynting vector.

Appendix C Rough surface criteria

Depending on the flatness of the reflecting surface, two types of reflection can be distinguished: specular and diffuse reflection.
Specular reflection is a reflection of the same type as caused by a smooth surface: it is directional and it obeys the laws of classical optics and its phase is coherent. The well known laws for reflection on flat surfaces, summarised in Appendix B, can be used. Diffuse scattering however, is a phenomenon that is dominant in case of reflection on rough surfaces. It has little directivity, its phase is incoherent and its fluctuations are large in amplitude.
The Rayleigh criterion establishes an approximate dividing line between truly rough surfaces and those that may be regarded as smooth.
The dividing line is based on a maximum phase shift that can occur due to two reflected waves in a point (Figure C.1)

$$\Delta\phi = \frac{4\pi D}{\lambda} \cdot \sin\psi \qquad \text{(C.1)}$$

in which:

D: Average depth of irregularity [m],
λ: Wavelength [m],
$\Delta\phi$: Phase difference [rad],
ψ: Grazing angle [rad].

To distinguish between a flat and a rough surface, Rayleigh proposed the criterion of $\Delta\phi=\pi/2$. Other values of $\Delta\phi$ like $\Delta\phi=\pi/8$ have been called more realistic [5]. Based on $\Delta\phi=\pi/8$ the flat-rough dividing line for average depth of irregularity can be defined by:

$$D < \frac{\lambda}{32\sin\psi} \text{ flat surface;} \qquad \text{(C.2)}$$

$$D > \frac{\lambda}{32\sin\psi} \text{ rough surface.} \qquad \text{(C.3)}$$

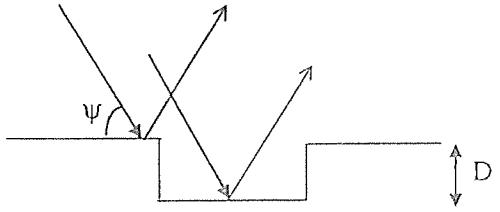

Figure C.1: Reflection on irregular surface.

Appendix D Determination of aperture illumination

The near-field correction factors for gain and beamwidth depend on the type of antenna illumination and the distance from the antenna [1],[3],[4].
If the antenna aperture illumination is unknown, it can be estimated by the 3 dB (far-field) beamwidth using the equation:

$$R = \frac{B \cdot L}{\lambda} \tag{D.1}$$

in which:

R = factor to determine illumination [rad],
B = Beamwidth at 3 dB points (horizontal or vertical) [rad],
L = horizontal or vertical dimension of antenna [m],
λ = wavelength [m].

The ANSI standard C95.3 [2] gives guidelines for estimating the illumination of rectangular and circular apertures (Tables D.1 and D.2).

Table D.1: Guidelines for rectangular aperture illumination

Limits of R	Estimated illumination F(x) (a = dimension aperture (m))
0.88-1.2	1 (uniform)
1.2-1.45	$\cos(\pi x/a)$
1.45-1.66	$\cos^2(\pi x/a)$
1.66-1.93	$\cos^3(\pi x/a)$

Table D.2: Guidelines for circular apertures illumination

Limits of R	Estimated illumination F(r). (q=2r/D; D=diameter (m) r = radius(m))
1.02-1.27	1 (uniform)
1.27-1.47	$(1-q^2)^1$
1.47-1.65	$(1-q^2)^2$
1.65-1.81	$(1-q^2)^3$

Appendix E Measurement errors

On december 1th, 1998 the NLR laboratory validated the TNO HI-4456 probe by performing a substitution measurement using a calibrated NLR probe as a substitute. Together with the probe calibration reports, probe factors were checked. The probe factors of the ECW probe HI-4450 were derived from the NLR and TNO probe by substitution.

The calibration status of the probes at december 1th 1998 were as follows:
NLR probe, Holady HI-34450, serial number 95442, calibration valid due to 17-02-1999
TNO probe, Holaday HI-4456, serial number 97982, calibration valid due to 16-11-1999
ECW probe, Holaday HI-4450, serial number 95440, calibration valid due to 09-01-1998

Measurement errors of the (TNO) HI4456 probe at 10 GHz are given in table E.1. The overall measurement errors of the ECW probe are equal to the overall measurement errors of the TNO probe. This is due to the adjustment of the respectively correction factors.

Tabel E.1 Measurement errors for HI-4456 probe.

Measurement error of (TNO) HI-4456 at 10 GHz (probe rotation angle adjusted for maximum sensitivity)					
	Error		Range		
	Min	Max	100 V/m	300 V/m	1000 V/m
Linearity 1 (according to cal. report)	-0.5 dB of full scale	+0.5 dB of full scale			
Linearity 2 (according to cal. report)	-2LSB	+2 LSB			
Isotropicity (measured at NLR at 10 GHz)	- 0.3 dB	+ 0 dB			
TOTAL	-0.8 dB -2LSB	+0.5 dB +2LSB	-9 V/m +6 V/m	-27 V/m +18 V/m	-90 V/m +60 V/m

REPORT DOCUMENTATION PAGE
(MOD-NL)

1. DEFENCE REPORT NO (MOD-NL)	2. RECIPIENT'S ACCESSION NO	3. PERFORMING ORGANIZATION REPORT NO
TD99-0279		FEL-99-A224
4. PROJECT/TASK/WORK UNIT NO	**5. CONTRACT NO**	**6. REPORT DATE**
28880	A99D818	December 1999
7. NUMBER OF PAGES	**8. NUMBER OF REFERENCES**	**9. TYPE OF REPORT AND DATES COVERED**
68 (incl appendices, excl RDP & distribution list)	8	Final

10. TITLE AND SUBTITLE

Electric field intensity levels near the HAWK system

11. AUTHOR(S)

[redacted]

12. PERFORMING ORGANIZATION NAME(S) AND ADDRESS(ES)

TNO Physics and Electronics Laboratory, PO Box 96864, 2509 JG The Hague, The Netherlands
Oude Waalsdorperweg 63, The Hague, The Netherlands

13. SPONSORING AGENCY NAME(S) AND ADDRESS(ES)

Military Medical Service Agency
Koningin Marialaan 17, PO Box 20701, 2500 ES The Hague, The Netherlands

14. SUPPLEMENTARY NOTES

The classification designation Ongerubriceerd is equivalent to Unclassified, Stg. Confidentieel is equivalent to Confidential and Stg. Geheim is equivalent to Secret.

15. ABSTRACT (MAXIMUM 200 WORDS (1044 BYTE))

Due to concern among Airforce personnel about the supposed relationship between health disorders and the exposure to electromagnetic fields due to radiators of the HAWK system, TNO-FEL was sponsored by the Netherlands Defense organisation to investigate the electric field intensities on the site of a HAWK installation. To determine the electric field intensity near the HAWK system, in December 1998 measurements have been performed on the HIPIR and the CWAR radars, which are part of the HAWK installation at Twenthe Air Base. To support the measurements and to be able to inter- and extrapolate the results a theoretical analysis was made. The measurement results turned out to be in good conformity with the theory.
Both measurement and theoretical results were compared to the STANAG 2345 (edition-2, 1997) exposure limits.

16. DESCRIPTORS	IDENTIFIERS
Radiation hazards Radar and antennas	HAWK

17a. SECURITY CLASSIFICATION (OF REPORT)	17b. SECURITY CLASSIFICATION (OF PAGE)	17c. SECURITY CLASSIFICATION (OF ABSTRACT)
[redacted]	Ongerubriceerd	Ongerubriceerd

18. DISTRIBUTION AVAILABILITY STATEMENT	17d. SECURITY CLASSIFICATION (OF TITLES)
Subject to approval MOD-NL	Ongerubriceerd

Distributielijst

1. DWOO
2. HWO-KM
3. HWO-KL
4. HWO-KLu
5. HWO-CO
6. DM&P TNO-DO
7. Directeur TNO-PML*
8. Directeur TNO-TM*
9. Accountcoördinator CO*
10. Bibliotheek KMA
11. Directeur-Generaal Personeel
12. Directeur Militair Geneeskundig Facilitair Bedrijf
13. Hoofd Gezamenlijke Geneeskundige Beleidsstaf
14. [redacted] arts
15. [redacted]
16. Documentatie MGFB
17. Reserve MGFB

18-32. Archief MGFB

33. Hoofd Afdeling Arbodienstverlening Koninklijke Luchtmacht
34. Hoofd Afdeling Grond-Lucht Geleide Wapens

35-36. Documentatie Arbodienstverlening KLu

37-38. Reserve Arbodienstverlening KLu

39-52. Archief Arbodienstverlening KLu

53. Directeur TNO-FEL
54. Adjunct-directeur TNO-FEL, daarna reserve
55. Archief TNO-FEL, in bruikleen aan MPC*
56. Archief TNO-FEL, in bruikleen aan Accountmanager CO
57. Archief TNO-FEL, in bruikleen aan [redacted]
58. Archief TNO-FEL, in bruikleen aan
59. Archief TNO-FEL, in bruikleen aan
60. Archief TNO-FEL, in bruikleen aan
61. Archief TNO-FEL, in bruikleen aan
62. Archief TNO-FEL, in bruikleen aan
63. Archief TNO-FEL, in bruikleen aan
64. Archief TNO-FEL, in bruikleen aan
65. Documentatie TNO-FEL
66. Reserve

Indien binnen de krijgsmacht extra exemplaren van dit rapport worden gewenst door personen of instanties die niet op de verzendlijst voorkomen, dan dienen deze aangevraagd te worden bij het betreffende Hoofd Wetenschappelijk Onderzoek of, indien het een K-opdracht betreft, bij de Directeur Wetenschappelijk Onderzoek en Ontwikkeling.

* Beperkt rapport (titelblad, managementuittreksel, RDP en distributielijst).